Cross-Section Measurements for Novel Medical Radionuclides at UCB/LBNL: The Challenge of "Simple" Experiments

Andrew S. Voyles

12 February 2018 – NE Department Colloquium

Berkeley
UNIVERSITY OF CALIFORNIA

Overview

- Background & history of nuclear medicine
- ^{64}Cu and ^{47}Sc (n,p) cross-section measurements
- Stacked-target charged particle excitation functions
- Path forward

Background & History of Nuclear Medicine

Nuclear Medicine in the U.S.

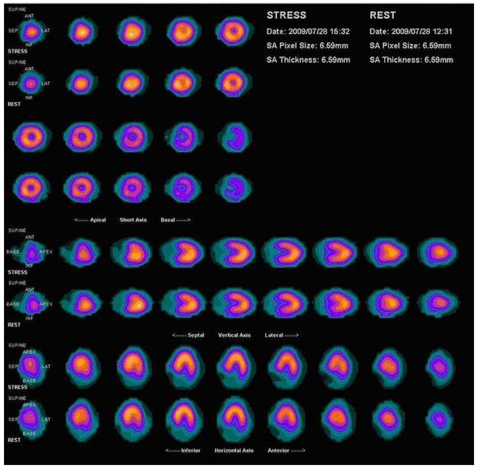

- Nearly 17M procedures performed annually in the US
- Major isotopes in modern clinical nuclear medicine:
    - ^{99m}Tc
        - Diagnostic isotope for cardiac, renal, lung function, tumor imaging
        - Produced as fission product in thermal reactors
        - Costs per 10-mCi dose ranges $20-40[1]
    - ^{18}F
        - PET isotope used for metabolic tumor & metastasis imaging
        - Produced by K~15 medical cyclotrons via $^{18}O(p,n)^{18}F$
        - Costs per 5-mCi dose ranges $400-800[2]
    - ^{131}I
        - β-therapy isotope used for treatment of cancers, including thyroid and neuroendocrine
        - Produced as fission product in thermal reactors
        - Costs per 200-mCi dose approximately $200[3]

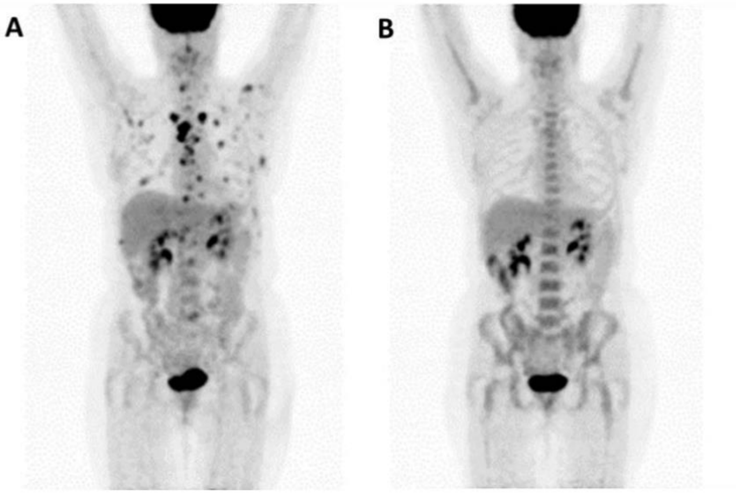

[1] C. Whipple and S. Larson, *Medical Isotope Production Without Highly Enriched Uranium*, 2009.
[2] United States Government Accountability Office and U.S. General Accounting Office, *Report GAO-08-452*,2008.
[3] A. N. Khalid, *et al*, "*Arch. Otolaryngol. Neck Surg.*, vol. 132, no. 3, pp. 244–250, 2006.

Nuclear Medicine in the U.S.

- Established medical radioisotopes face several challenges:
  - Non-ideal decay properties for desired application
    - Extra dose
    - Extra range
  - Curtailment of production facilities (^{99m}Tc)
  - Thermal reactor issues
    - Low yield
    - Difficult radiochemical purification
    - Feasibility & deployability

Why do we keep doing this?

How can we improve this?

Nuclear Medicine in the U.S.

- Established medical radioisotopes face several challenges:
  - Non-idea ... ion
    - Extra
    - Extra
  - Curtailment of production facilities (^{99m}Tc)
  - Thermal
    - Low
    - Diffic
    - Feasibility & deployability

Novel isotopes…

…and new paradigms for isotope production!

Why do we keep doing this?

How can we improve this?

Some perspective

S.M. Qaim

Some perspective

1. Charged-particle reactions for the production of medical isotopes at low energies (E < 30 MeV):
   - ^{45}Sc(p,n)^{45}Ti; ^{52}Cr(p,n)^{52}Mn; ^{54}Fe(d,n)^{55}Co; ^{67}Zn(p,α)^{64}Cu; ^{72}Ge(p,n)^{72}As, ^{74}Se(d,n)^{75}Br; ^{86}Sr(p,n)^{86}Y; ^{120}Te(p,n)^{120}I

^{32}S(n,p)^{32}P; ^{47}Ti(n,p)^{47}Ca, ^{64}Zn(n,p)^{64}Cu; ^{67}Zn(n,p)^{67}Cu; ^{89}Y(n,p)^{89}Sr, ^{105}Pd(n,p)^{105}Rh; ^{149}Sm(n,p)^{149}Pm, ^{153}Eu(n,p)^{153}Sm, ^{159}Tb(n,p)^{159}Gd; ^{161}Dy(n,p)^{161}Tb; ^{166}Er(n,p)^{166}Ho; ^{169}Tm(n,p)^{169}Er; ^{175}Lu(n,p)^{175}Yb; ^{177}Hf(n,p)^{177}Lu

4. Need small uncertainties on all dosimetry reactions

Highlight from WTTC 2016: ^{54}Fe(p,α)^{51}Mn

NDNCA Whitepaper available at http://bang.berkeley.edu/events/ndnca/whitepaper/

Berkeley UNIVERSITY OF CALIFORNIA

Some perspective

- Emerging trends for next-generation (targeted & personalized) nuclear medicine:
  - Targeted alpha therapy (5-10 MeV)
    - 40-80 μm range → single cell
  - Targeted Auger therapy (20 eV – 1 keV)
    - 1 nm – 2 μm → cellular nucleus
  - Theranostic medicine
    - Simultaneous imaging and therapy

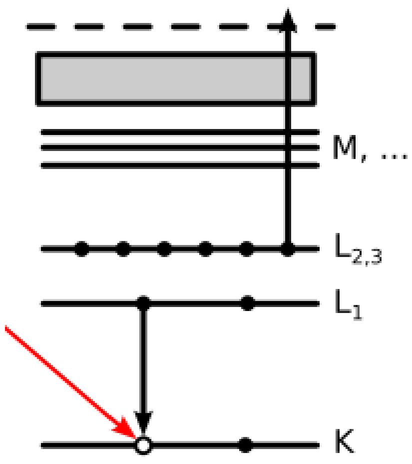

Overview

- Ongoing targeted experimental campaign to address these needs:
  - (n,p) production cross sections – UCB
  - Stacked-target charged particle excitation functions
    - Low energy – LBNL
    - Moderate energy – LANL
    - Bonus – spin distribution of excited nuclear states

The LBNL/UCB Bay Area Nuclear Data (BAND) Group*…

A. Voyles

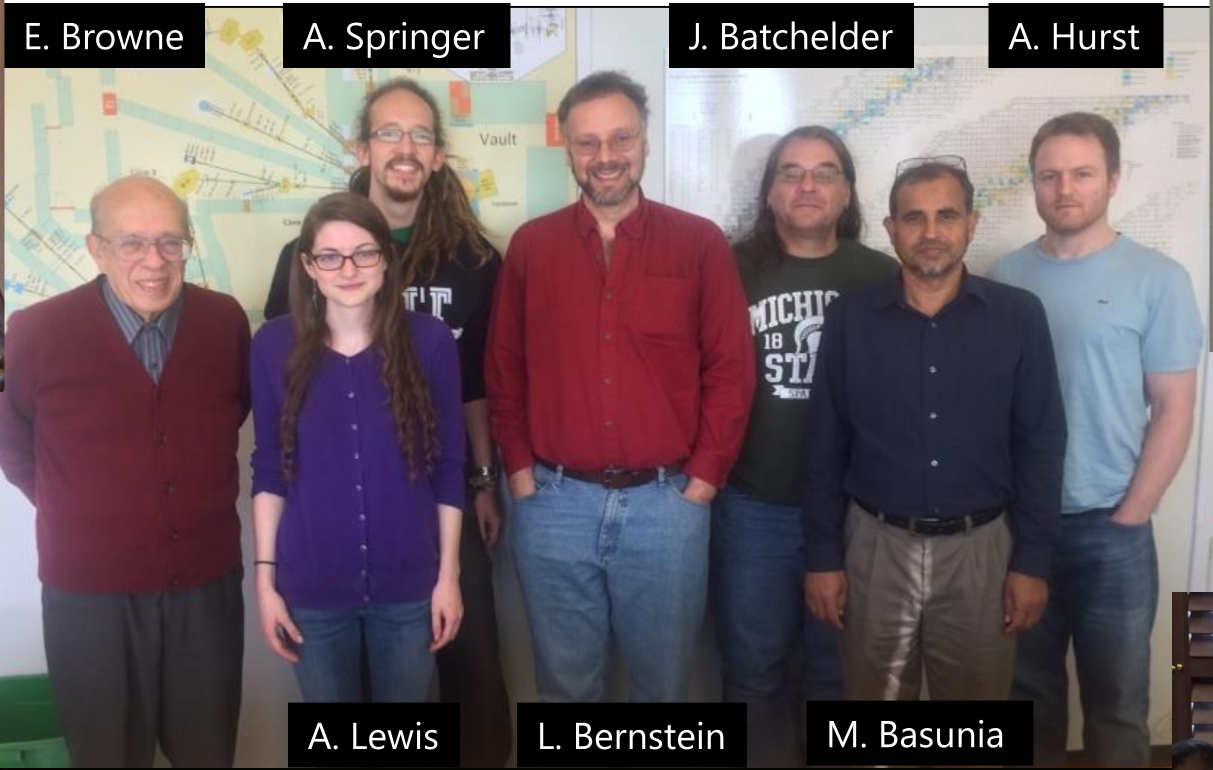

J. Morrell

L. Kirsch

E. Matthews

Our goal is to address the data needs of the applied nuclear science community while training the next generation of nuclear scientists and engineers in the process

Berkeley
UNIVERSITY OF CALIFORNIA

UCB Nuclear Engineering students lead our experimental program

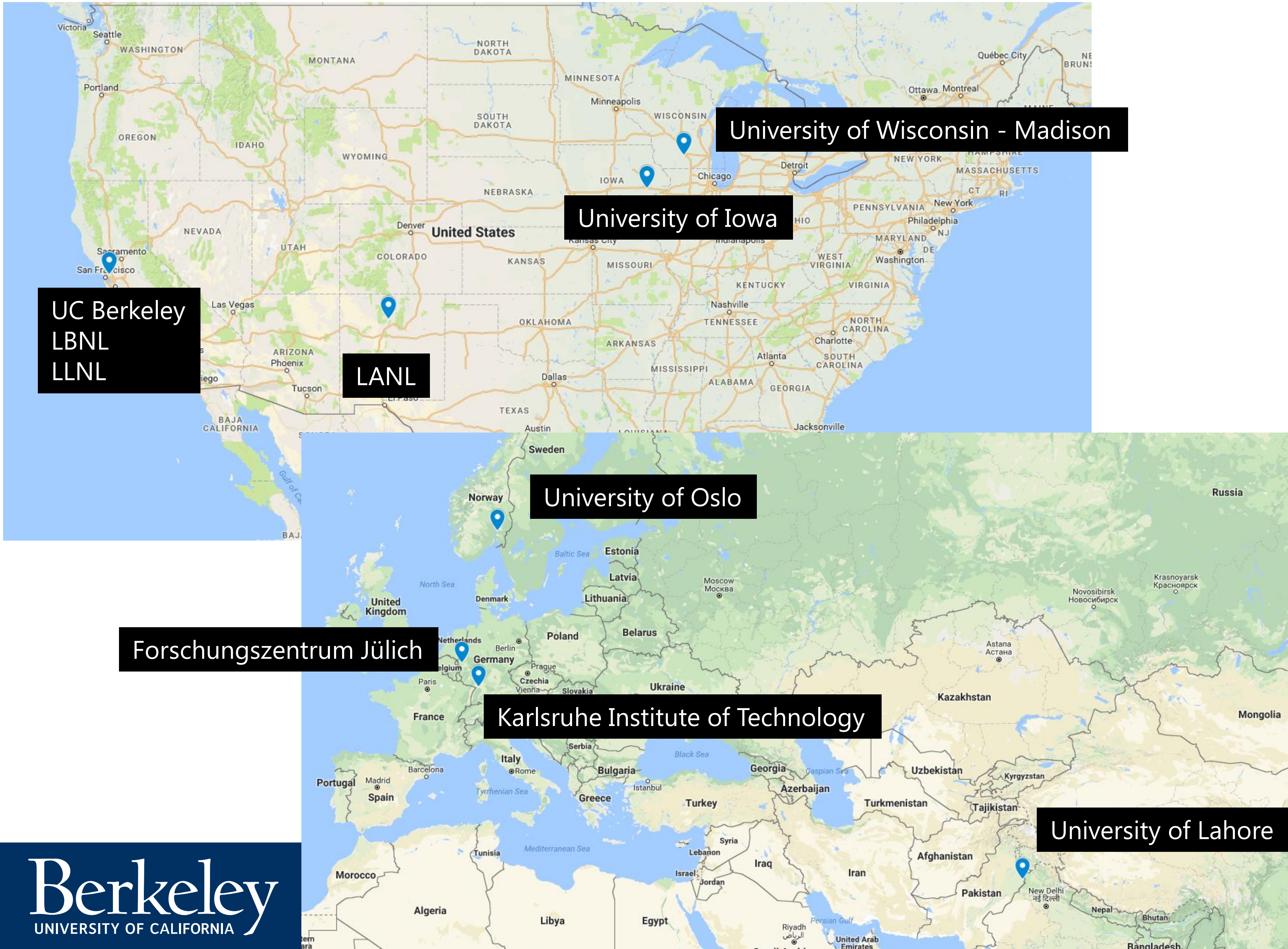

Berkeley
UNIVERSITY OF CALIFORNIA

A simple picture of cross-sections…

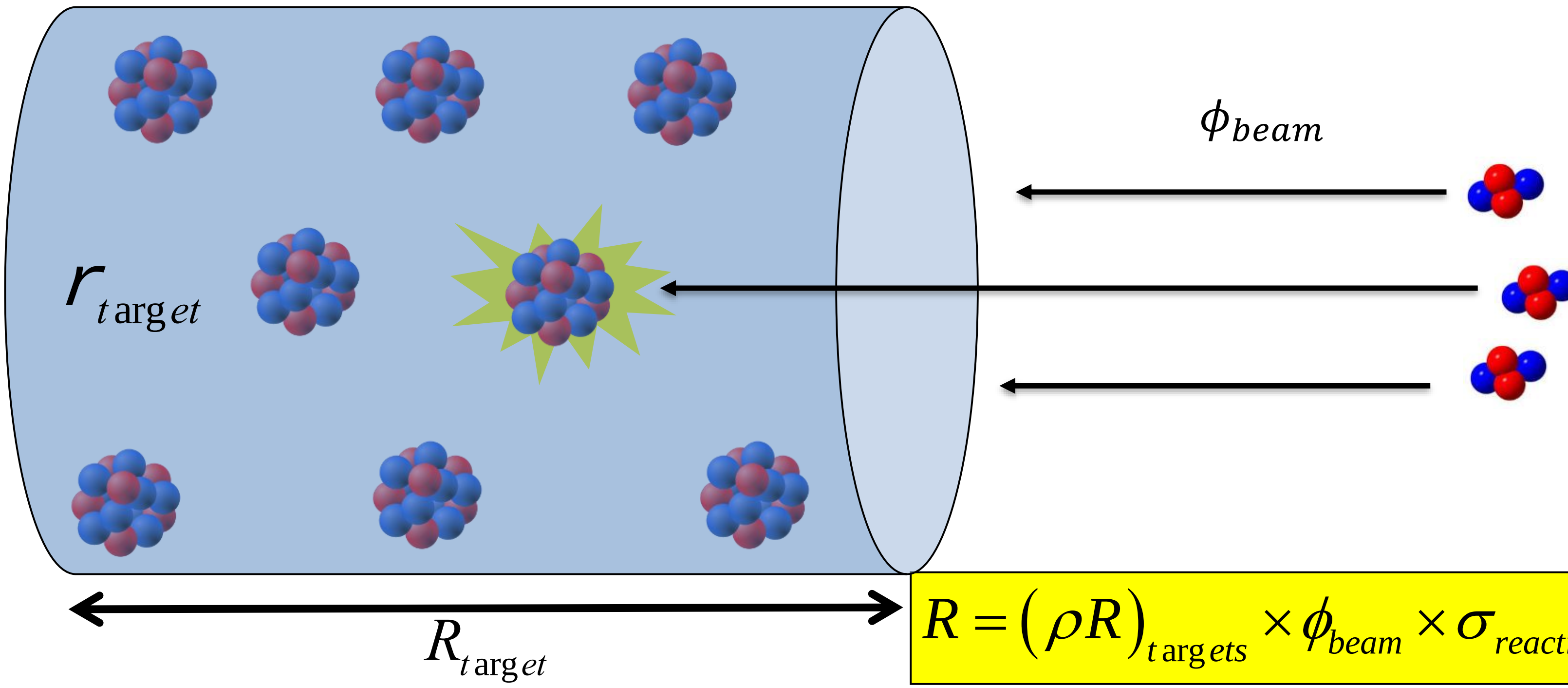

$$R = (\rho R)_{targets} \times \phi_{beam} \times \sigma_{reaction}$$

Proper characterization of ϕ_{beam} is often the largest source of uncertainty in precision measurements

^{64}Cu and ^{47}Sc (n,p) Cross-Section Measurements

Medical Applications

- Emerging medical radionuclides
  - ^{64}Cu ($t_{1/2}$ = 12.7 hr) – 61% β^+ to ^{64}Ni, 39% β^- to ^{64}Zn
  - ^{47}Sc ($t_{1/2}$ = 3.35 d) – β^- to ^{47}Ti, with 159-keV γ

Promising Prospects for ^{44}Sc-/^{47}Sc-Based Theragnostics: Application of ^{47}Sc for Radionuclide Tumor Therapy in Mice

Cristina Müller[1], Maruta Bunka[2,3], Stephanie Haller[1], Ulli Köster[4], Viola Groehn[5], Peter Bernhardt[6,7], Nicholas van der Meulen[2], Andreas Türler[2,3], and Roger Schibli[1,8]

[1]Center for Radiopharmaceutical Sciences ETH-PSI-USZ, Paul Scherrer Institute, Villigen-PSI, Switzerland; [2]Laboratory of Radiochemistry and Environmental Chemistry, Paul Scherrer Institute, Villigen-PSI, Switzerland; [3]Laboratory of Radiochemistry and Environmental Chemistry, Department of Chemistry and Biochemistry University of Bern, Bern, Switzerland; [4]Institut Laue-Langevin, Grenoble, France; [5]Merck and Cie, Schaffhausen, Switzerland; [6]Department of Radiation Physics, The Sahlgrenska Academy, University of Gothenburg, Gothenburg, Sweden; [7]Department of Medical Physics and Medical Bioengeneeri University Hospital, Gothenburg, Sweden; and [8]Department of Chemistry and Applied Biosciences, ETH Zuric

In Vivo Evaluation of Pretargeted ^{64}Cu for Tumor Imaging and Therapy

Michael R. Lewis, PhD[1]; Mu Wang, MD[1]; Donald B. Axworthy, BS[2]; Louis J. Theodore, PhD[2]; Robert W. Mallet, BS[2]; Alan R. Fritzberg, PhD[2]; Michael J. Welch, PhD[1]; and Carolyn J. Anderson, PhD[1]

[1]Mallinckrodt Institute of Radiology, Washington University School of Medicine, St. Louis, Missouri; and [2]NeoRx Corporation, Seattle, Washington

Why (n,p) via DD neutrons?

- Advantages over thermal reactors:
  - Co-production of many unwanted activities via (n,γ)
  - Far cheaper startup costs, no proliferation concerns
- Advantages over DT neutrons:
  - 14-15 MeV DT neutrons open up unwanted (n,pxn) channels, contaminating the desired product
  - No tritium handling concerns
- 2-3 MeV DD neutrons are ideal for (n,p) and (n,α) production, but often suffer from fairly low flux, and poor nuclear data

The UC Berkeley High Flux Neutron Generator

2.45 MeV neutrons, 10^7 n/s/cm^2
Extraction Plate: 5mm diameter

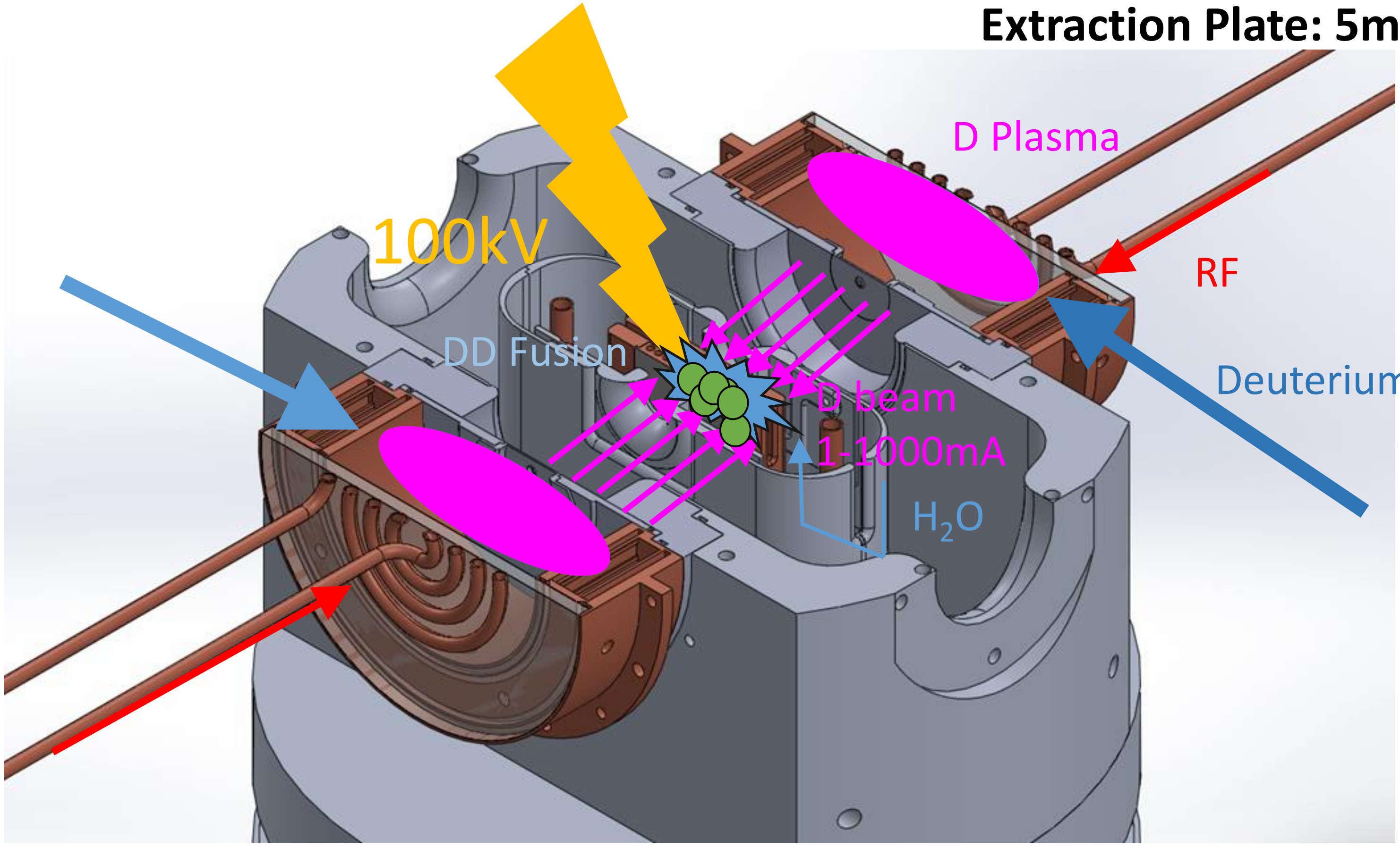

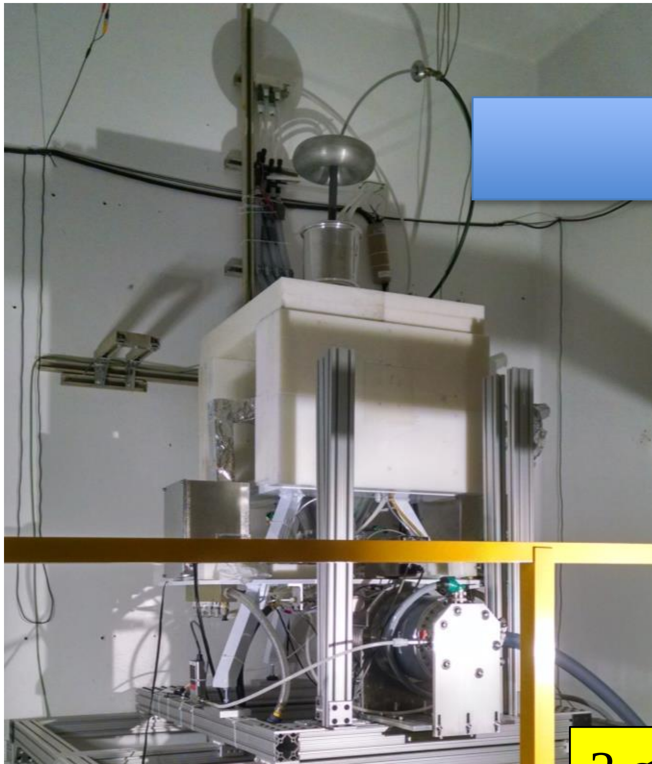


M. Unzueta

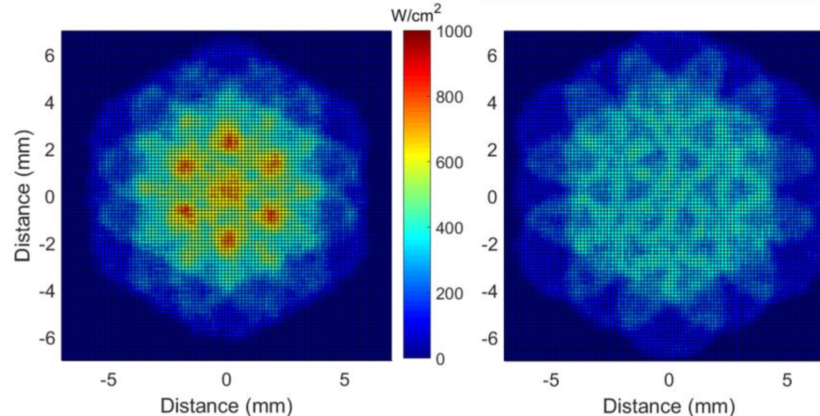

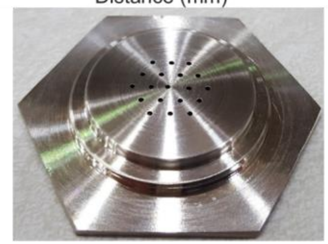

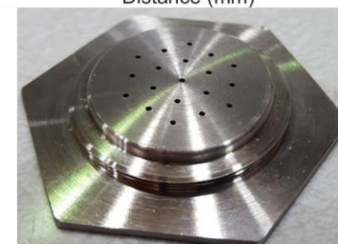

3 generations of our
“real neutron source”

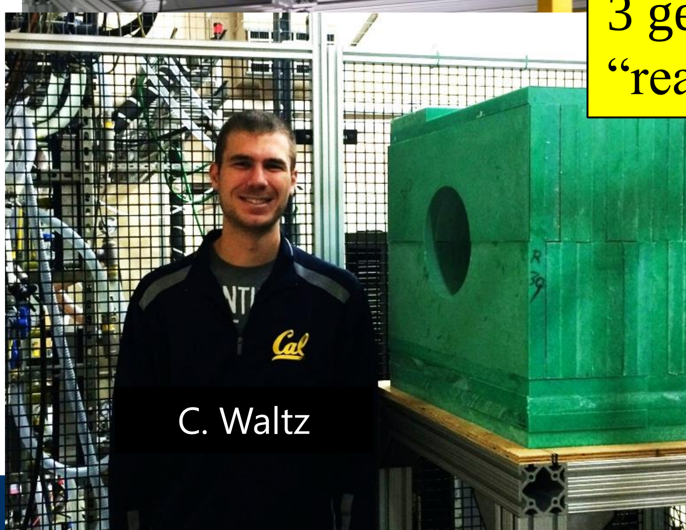
C. Waltz

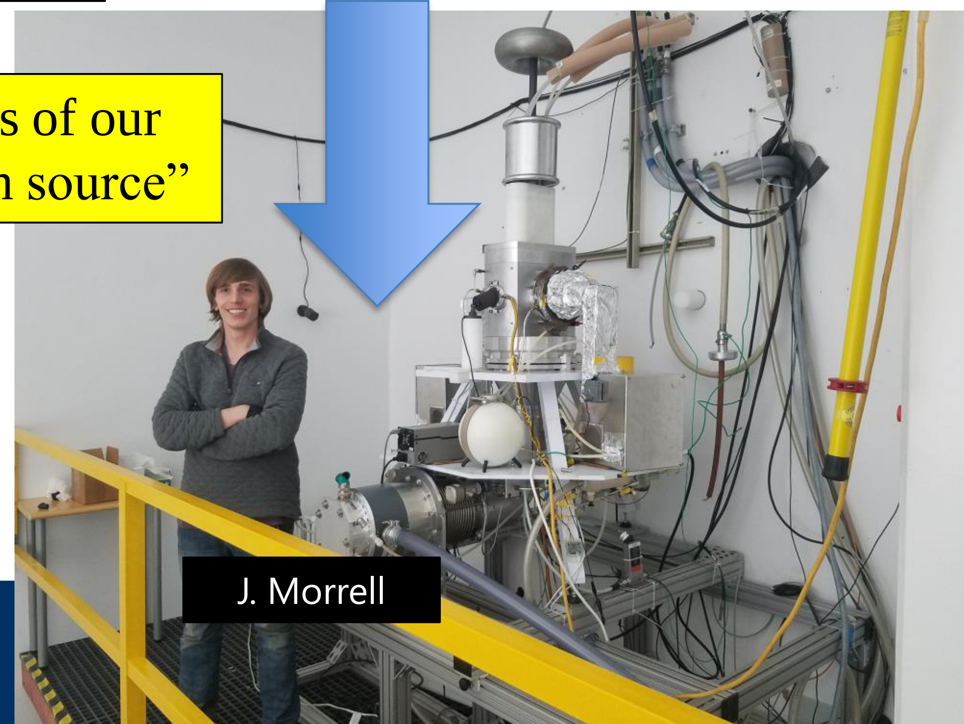
J. Morrell

The UC Berkeley High Flux Neutron Generator

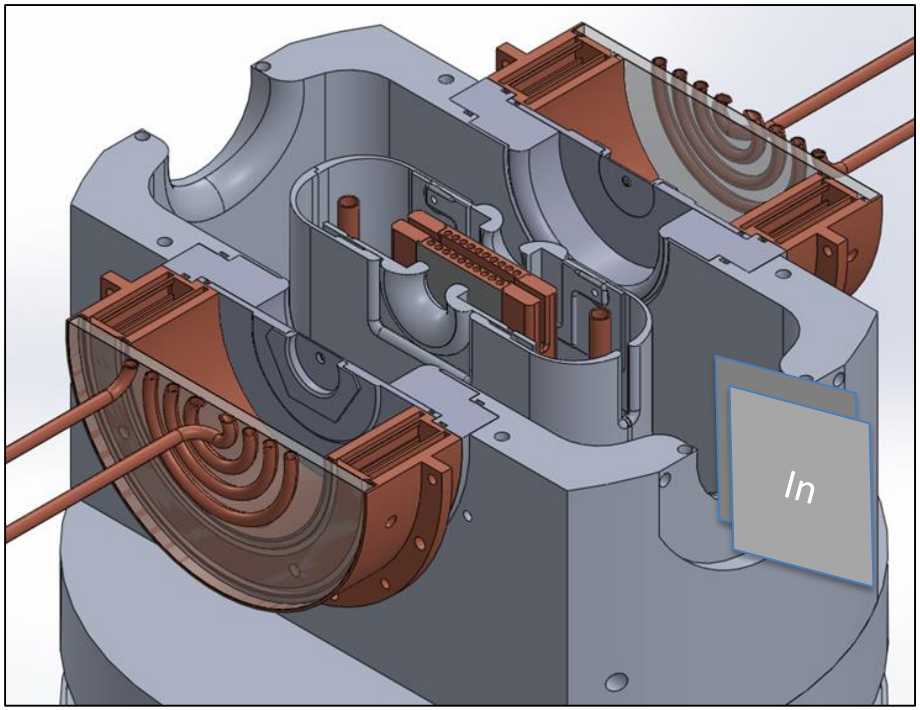

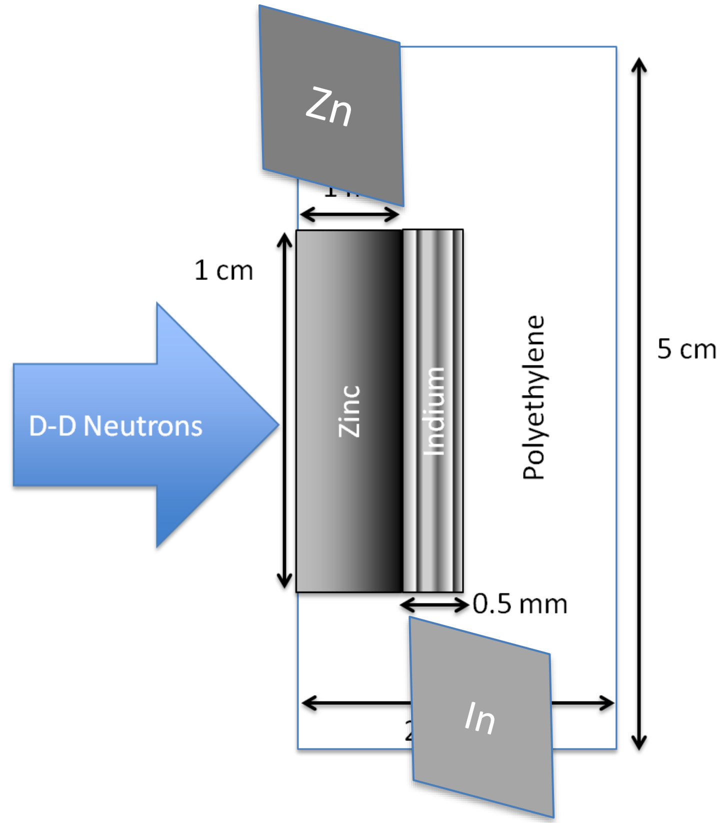

Relative Activation Measurements

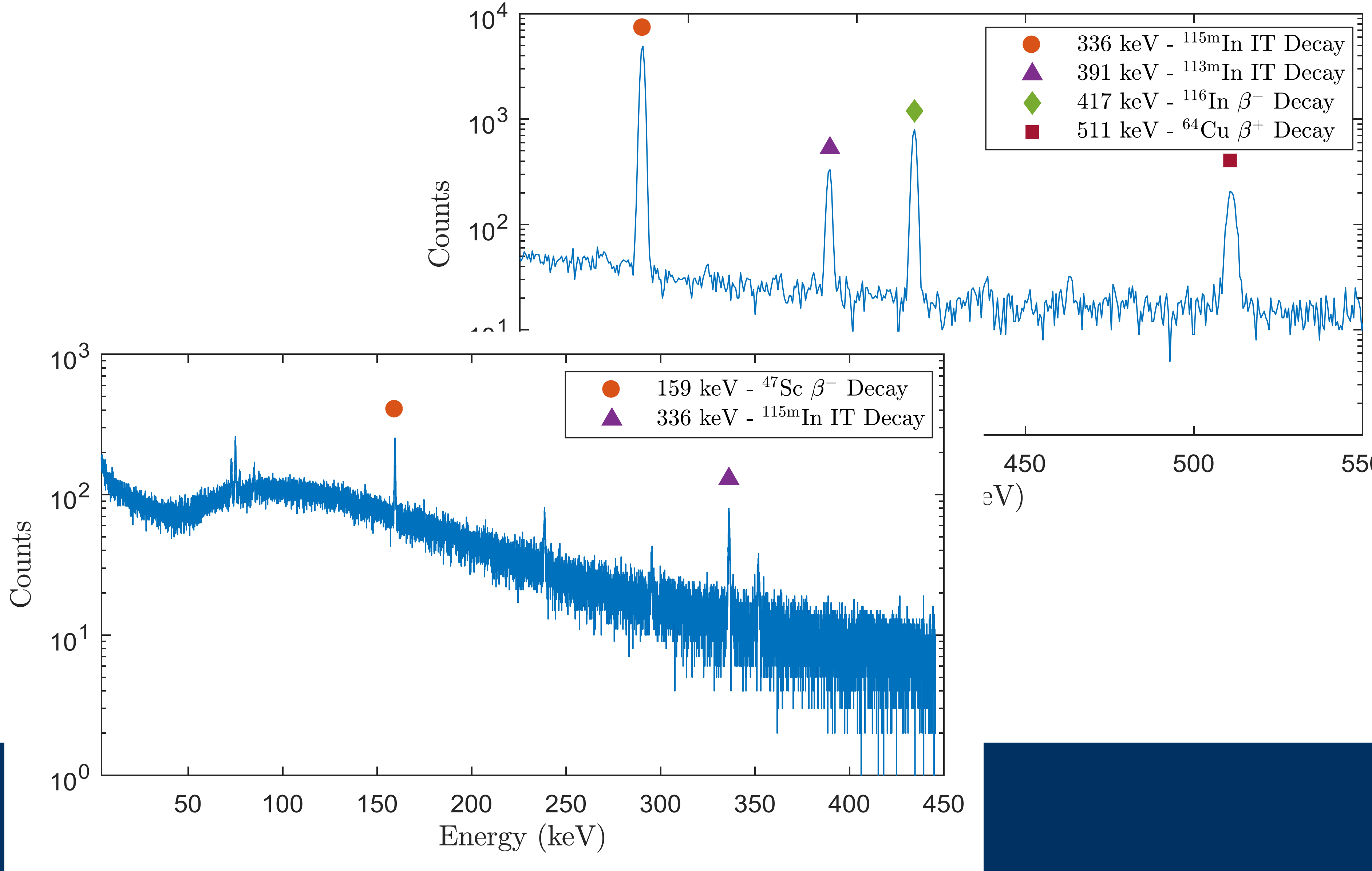

Relative Activation Measurements

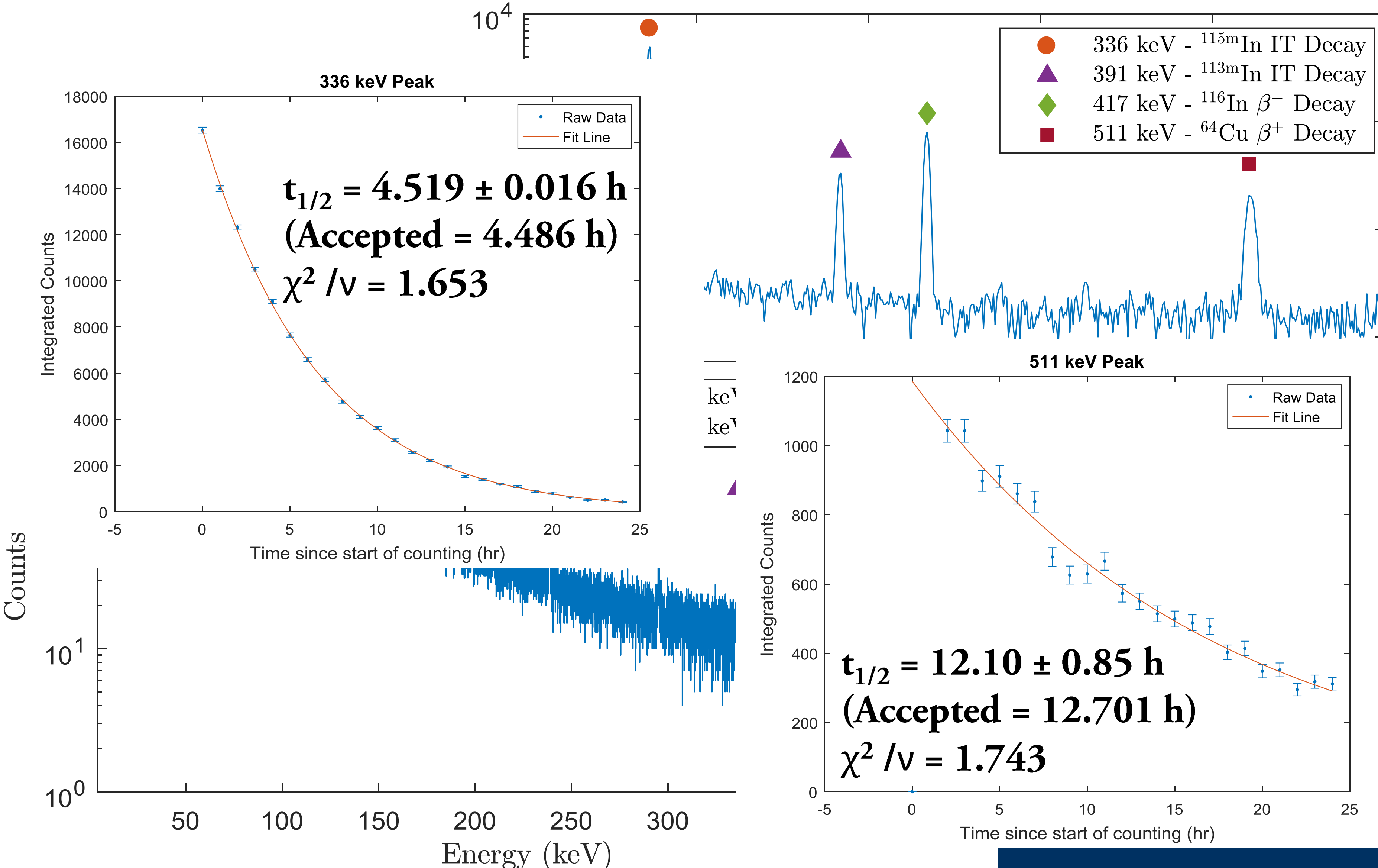

Neutron Energy Spread

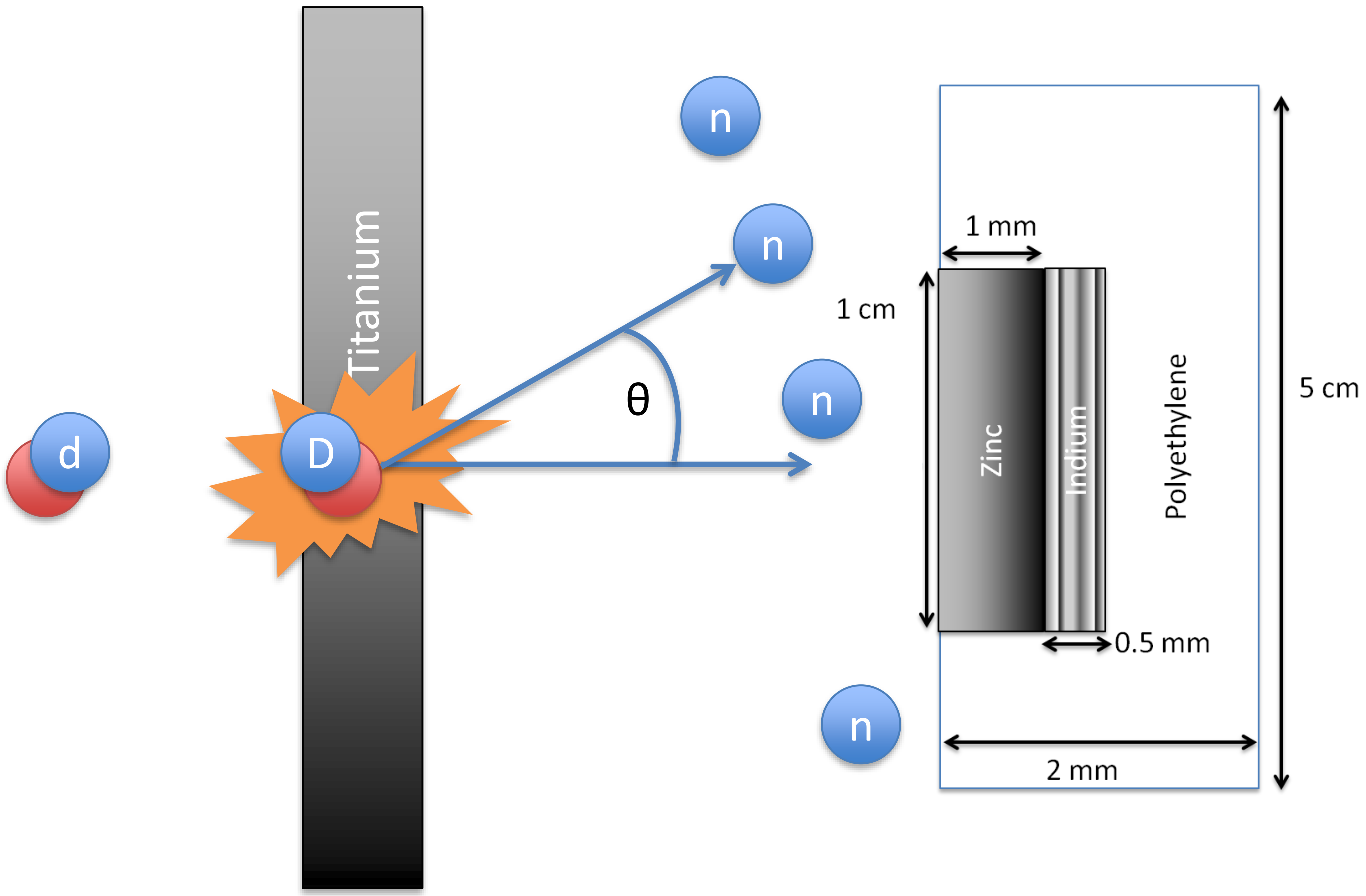

Neutron Energy Spread

H. Liskien *et al.*, Nucl Data Tables, vol 11, 2973

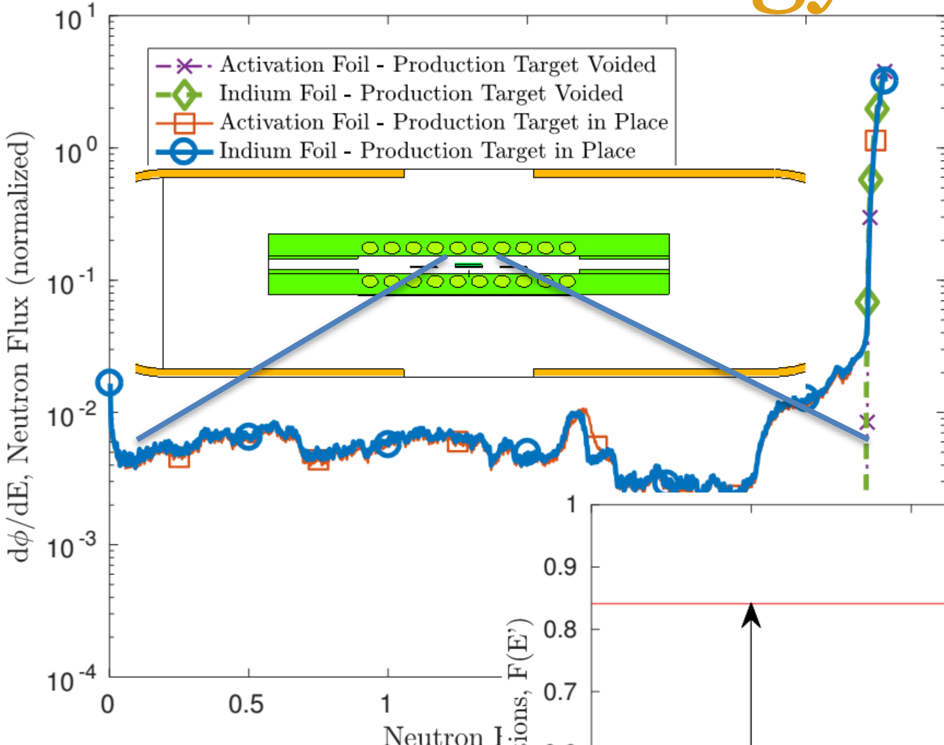

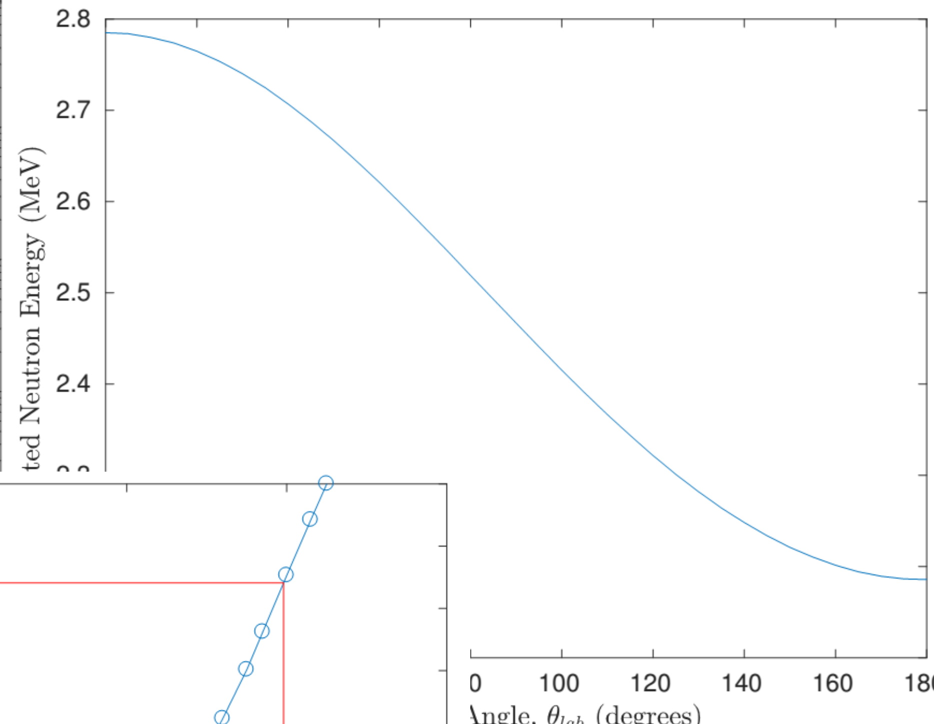

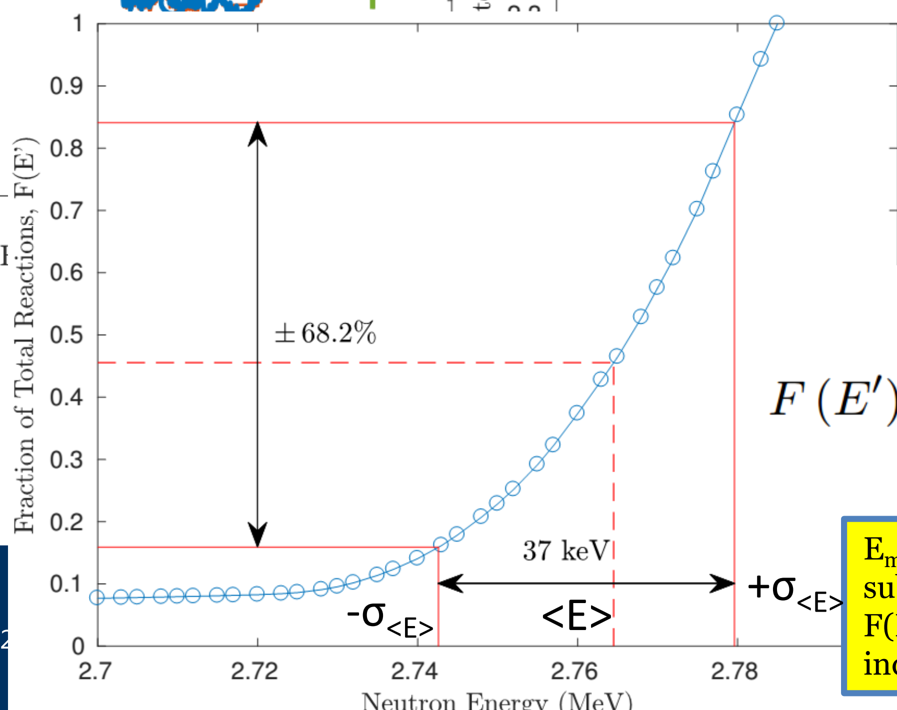

Neutron flux profile modeled in target and monitor foil, using MCNP6

$$F\left(E'\right) = \frac{\int_0^{E'} \sigma(E)\frac{d\phi}{dE}dE}{\int_0^{E_{max}} \sigma(E)\frac{d\phi}{dE}dE}$$

E_{max} = Maximum energy neutron subtended by foil
F(E') = Fraction of Total Reactions induced up to energy E'

Neutron Energy Spread

Table 3. Results of cross section measurement.

Reaction	$\sigma(E_n = 2.7645$ MeV$)$ (mb)
^{64}Zn(n,p)^{64}Cu (relative to ^{113}In)	45.953 ± 3.351, 46.493 ± 2.805, 46.9 ± 3.189
^{64}Zn(n,p)^{64}Cu (relative to ^{115}In)	49.716 ± 3.335, 49.011 ± 2.698,
^{47}Ti(n,p)^{47}Sc (relative to ^{115}In)	25.901 ± 1.7089,

^{64}Zn(n,p)^{64}Cu

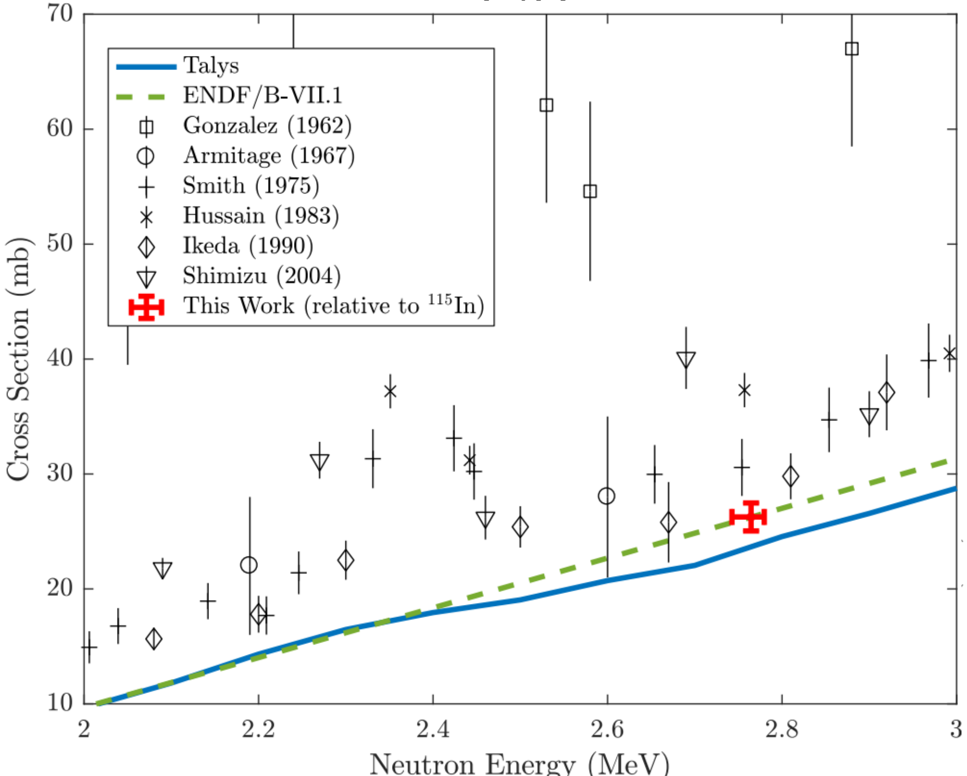

^{47}Ti(n,p)^{47}Sc

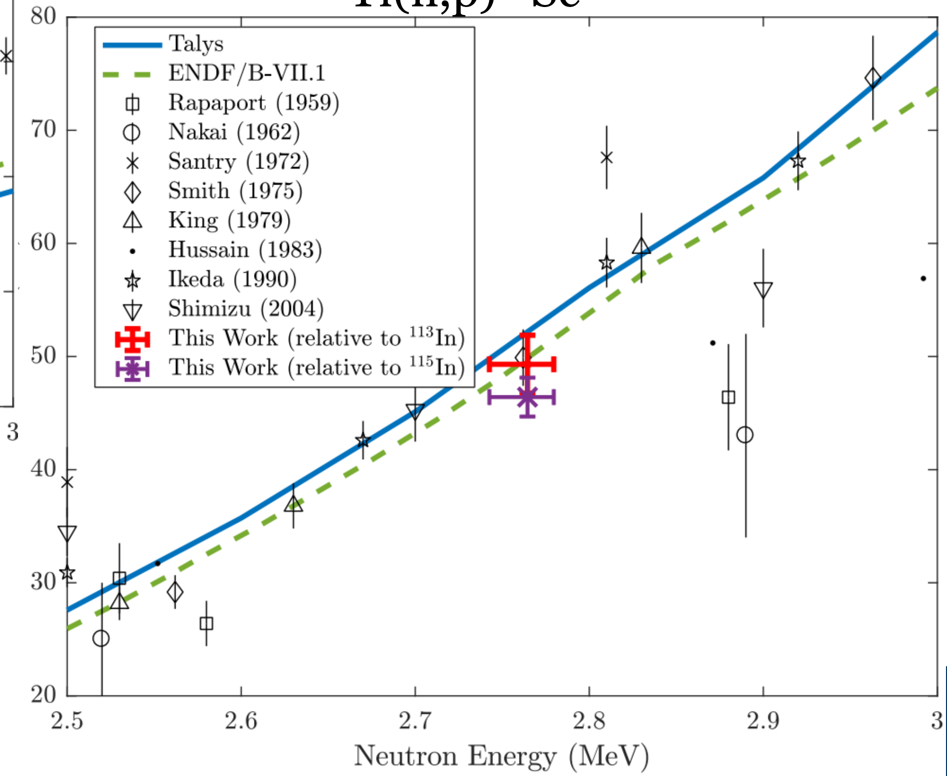

"Measurement of the ^{64}Zn, ^{47}Ti(n,p) cross sections using a DD neutron generator for medical isotope studies", Nuclear Instruments and Methods in Physics Research B 410 (2017) 230–239

Neutron Utilization

$$A(t_i) = \eta R_n \left(1 - e^{-\lambda t_i}\right)$$

- Theoretical saturation activities are currently estimated at 1.5 kBq of ^{64}Cu, 0.11 kBq of ^{47}Sc
  - Characterizes the effectiveness of a neutron generator as an isotope generator
  - Measured production rates were 453.8 Bq of ^{64}Cu, 31.6 Bq of ^{47}Sc
  - **Implies $\eta \approx 3 \times 10^{-5}$ (^{64}Cu), $\eta \approx 1 \times 10^{-5}$ (^{47}Sc)**

Measurement of the ^{98}Mo(n,γ) Cross Section

- A recent experiment at the HFNG was conducted by Eric Matthews to re-measure the (n,γ) cross section of ^{98}Mo.
- Using a custom target holder, four energy locations were measured.
- This cross section has not been measured since 1967 and re-measurement of this cross section in the 1-10 MeV was marked as a vital nuclear data need in the NDNCA nuclear data needs matrix, for thermal reactor ^{99}Mo production.

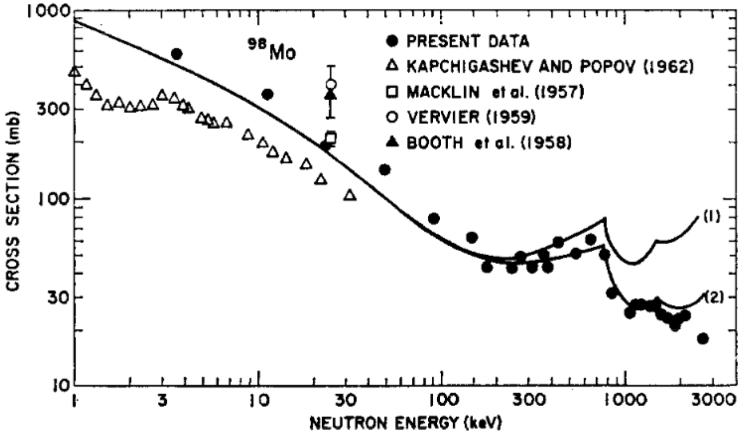

Stupegia et al., 1967

Stacked-target Charged Particle Excitation Functions

Low Energy – LBNL

Why charged particle production?

- Cyclotron
  - Many hospitals have small K~15 medical cyclotrons for PET tracer production
  - Leverage existing infrastructure
  - Explore higher energies for regional research cyclotrons, basic science
- Linac
  - Commonly used for high-energy production (LANL – IPF)
  - Useful for anchoring to complementary low-energy measurements

^{51,52}Mn - Motivation

- Emerging medical radionuclides
  - ^{51}Mn ($t_{1/2}$ = 46 min, 97% β^+) – short-lived PET tracer for metabolic studies
  - ^{52g}Mn ($t_{1/2}$ = 5.6 d, 29% β^+) – long-lived PET tracer for neuron tracking, immune studies

Preparation and *in vivo* characterization of $^{51}MnCl_2$ as PET tracer of Ca^{2+} channel-mediated transport

Stephen A. Graves[1], Reinier Hernandez[1], Hector F. Valdovinos[1], Paul A. Ellison[1], Jonathan W. Engle[1]* Todd E. Barnhart[1], Weibo Cai[1,2,3], Robert J. Nickles[1]*

  - Manganese has well-established biochemistry and uptake via DOTA-based chelation

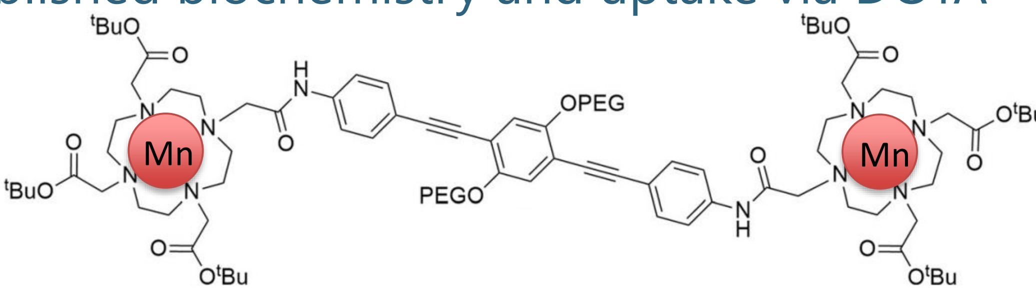

Almost no Fe(p,x) XS measurements exist – can use these to probe spin physics in the A≈50 region

Methodology

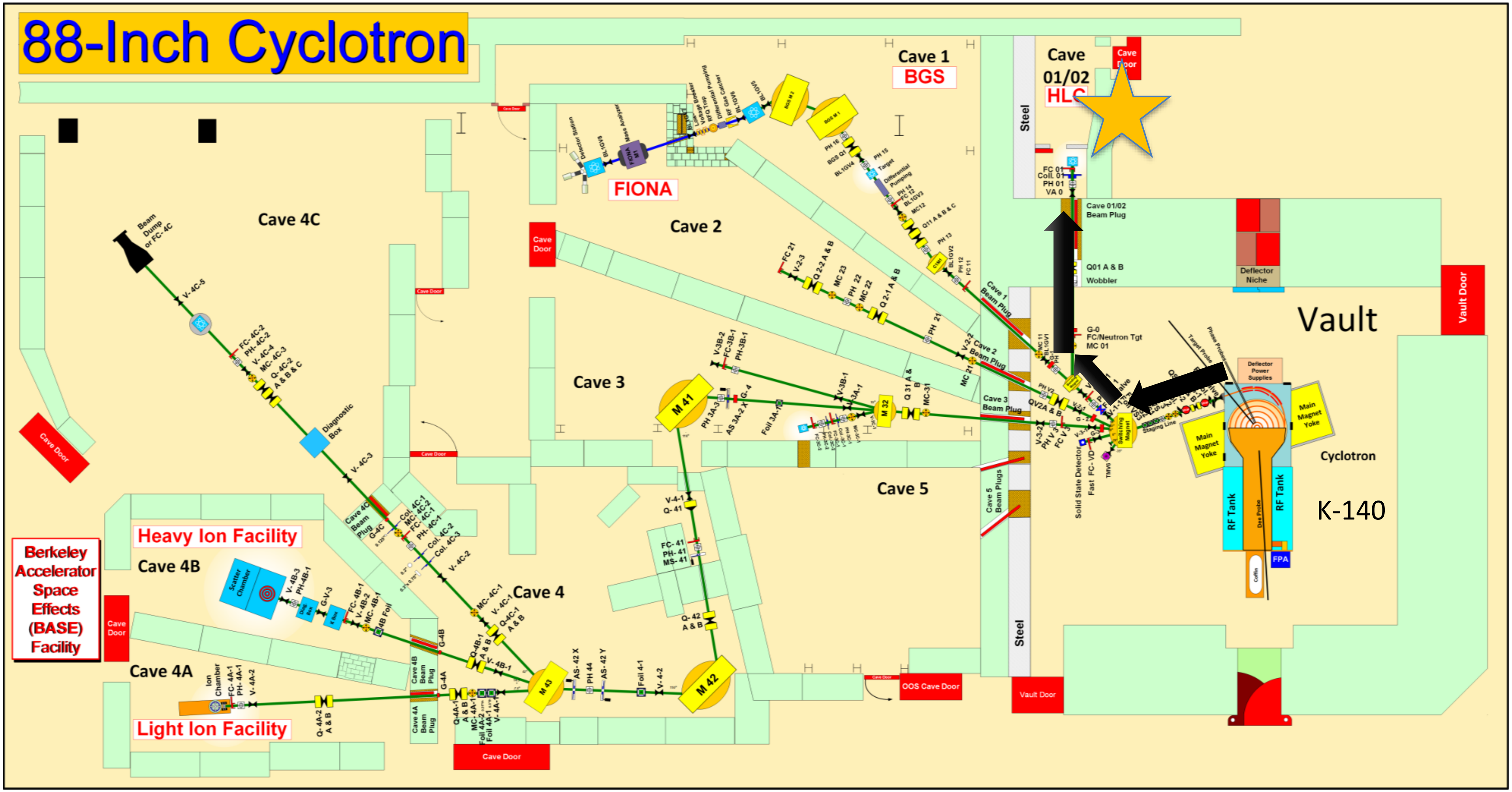

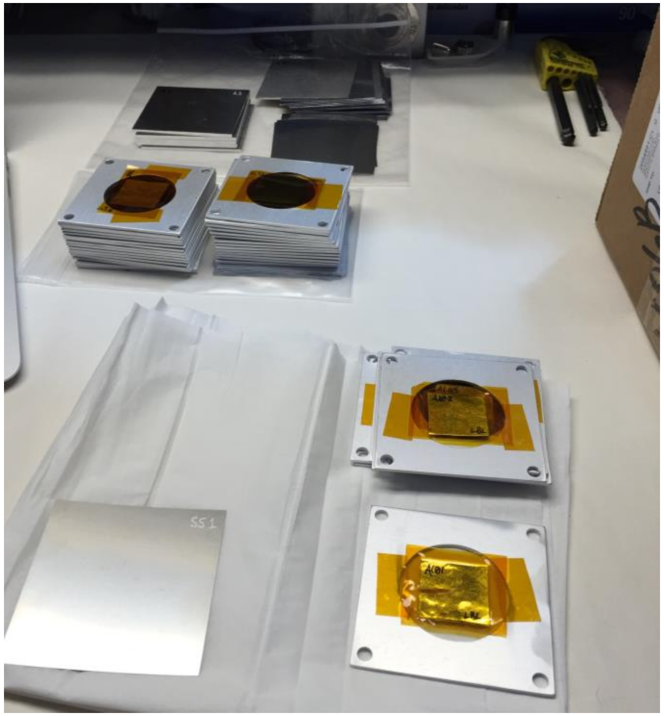

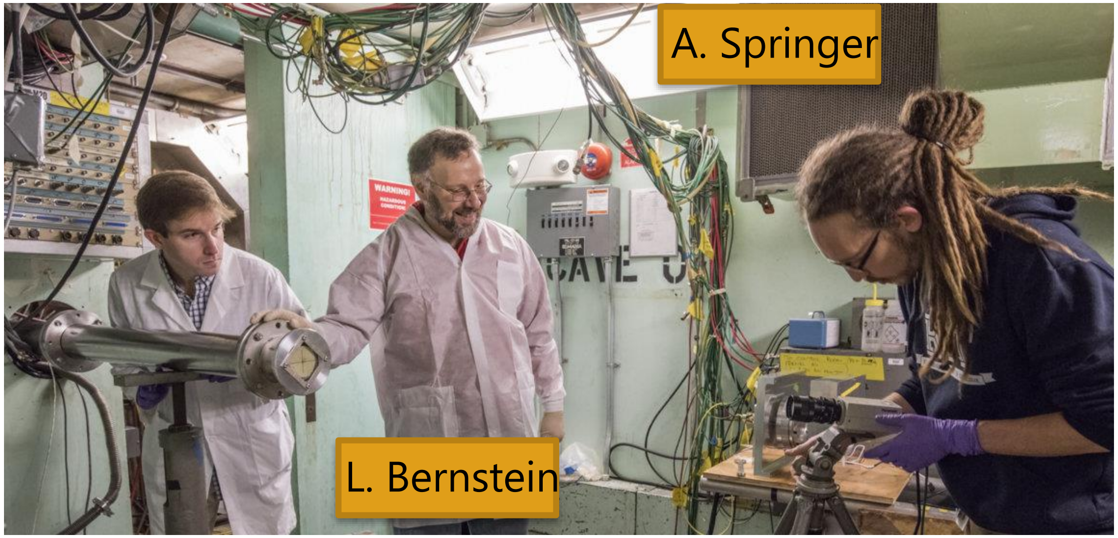

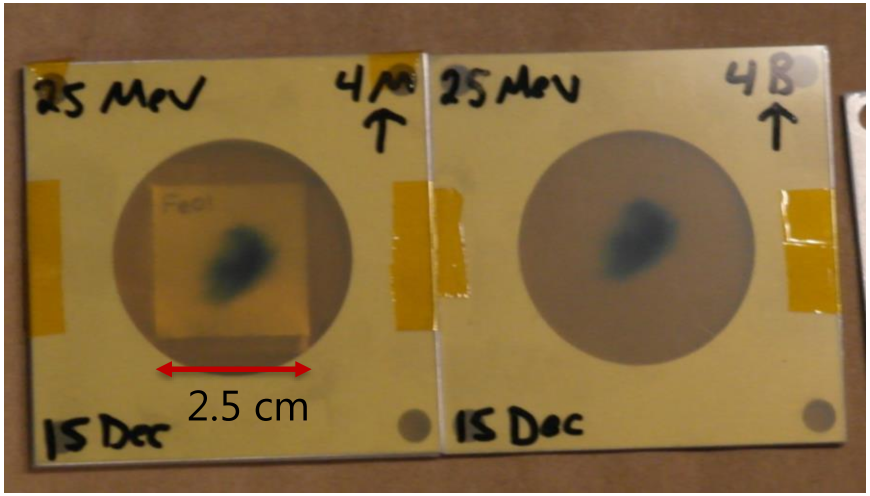

Two overlapping stacks:
E_p= 55→21 MeV, 25→11 MeV
(120 nA@10 min, 100 nA@20 min)

- 25 µm-thin ^{nat}Fe, ^{nat}Cu, ^{nat}Ti foils in 0.1” Al frames

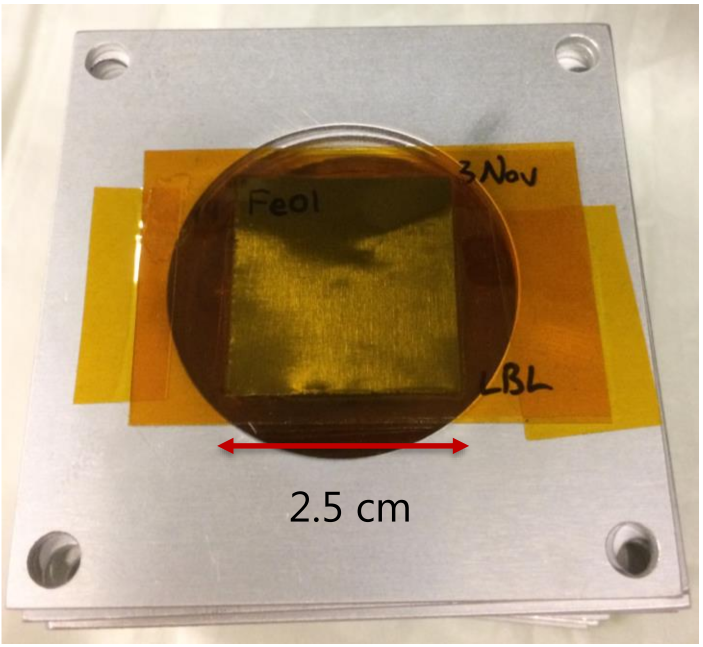

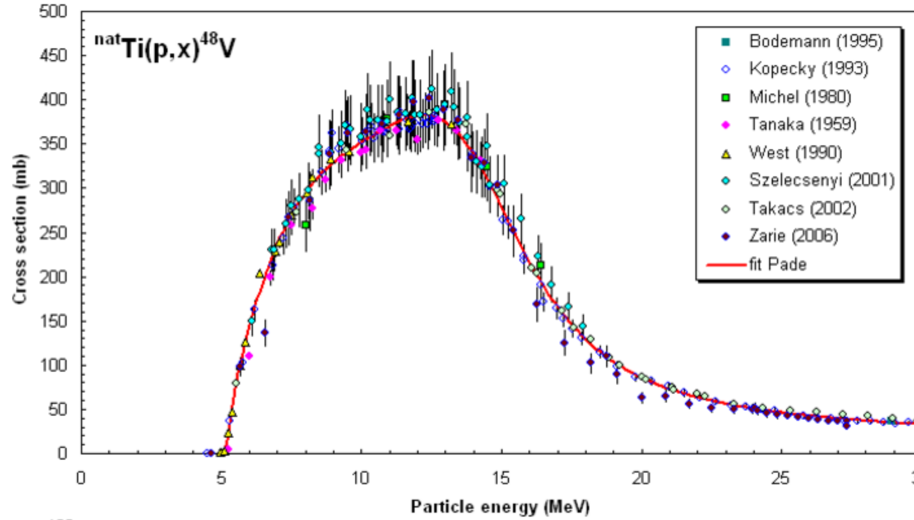

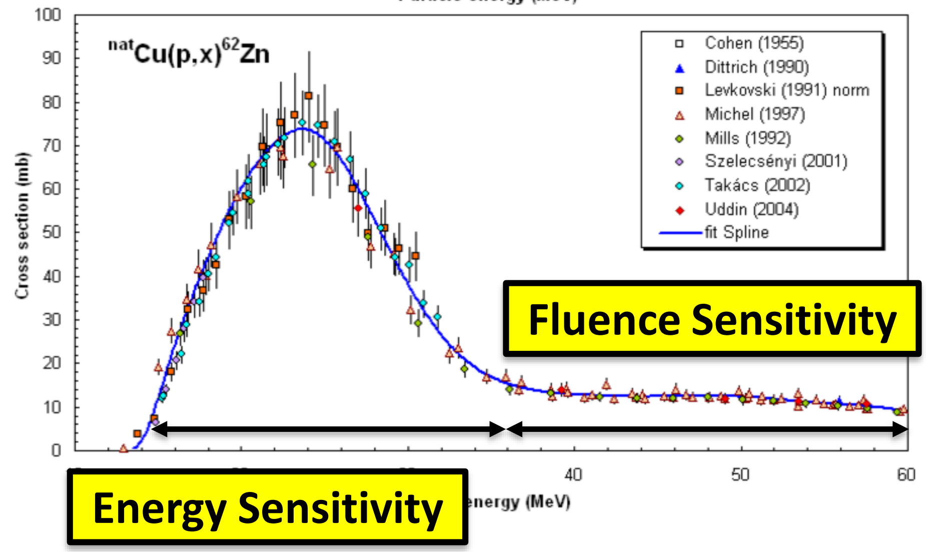

nds.iaea.org/medical/monitor_reactions.html

- Dosimetry: IAEA charged particle beam monitor reactions:
  - $^{nat}Ti(p,x)^{48}V$
  - $^{nat}Cu(p,x)^{62,63,65}Zn$

Data Analysis Issues

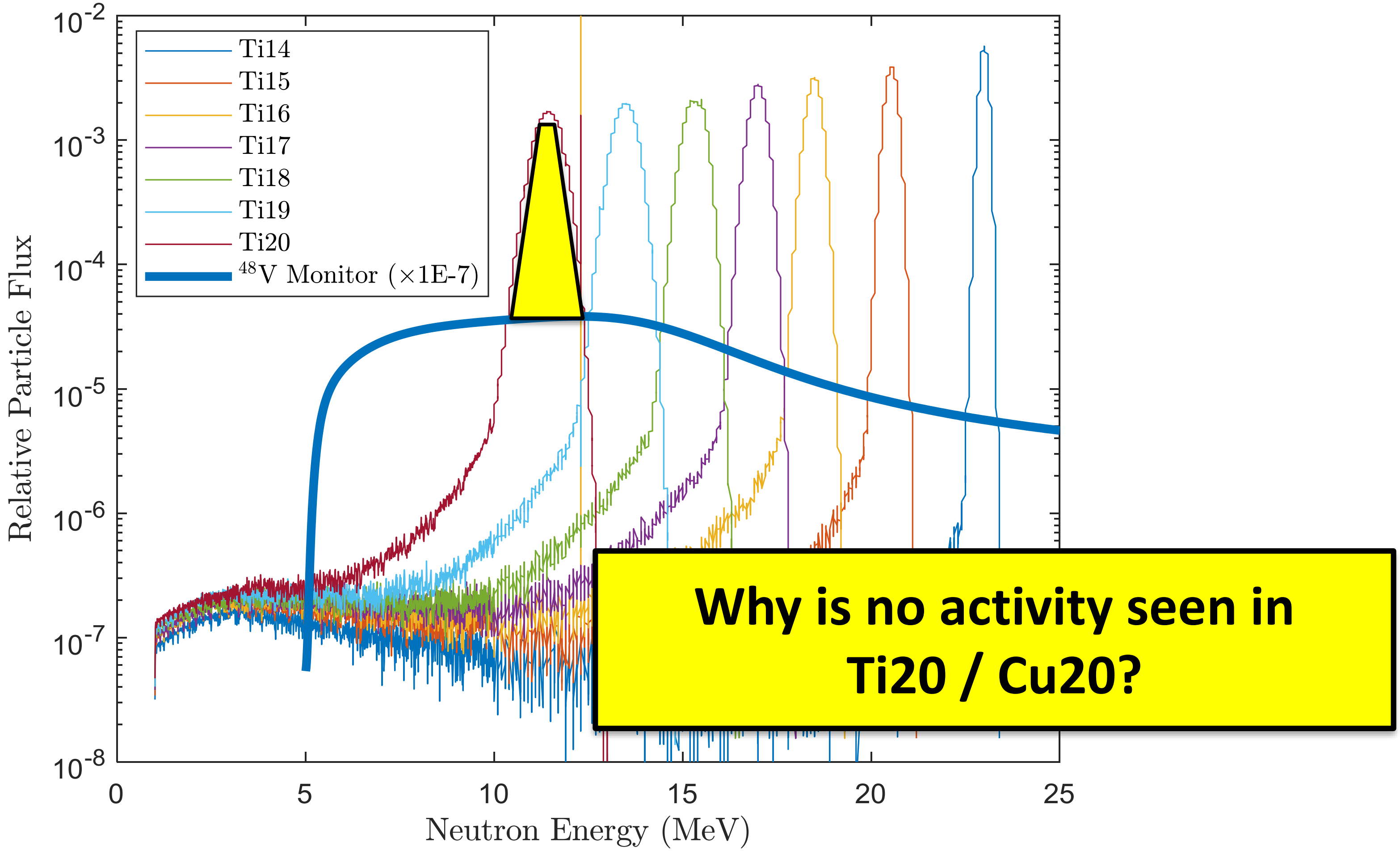

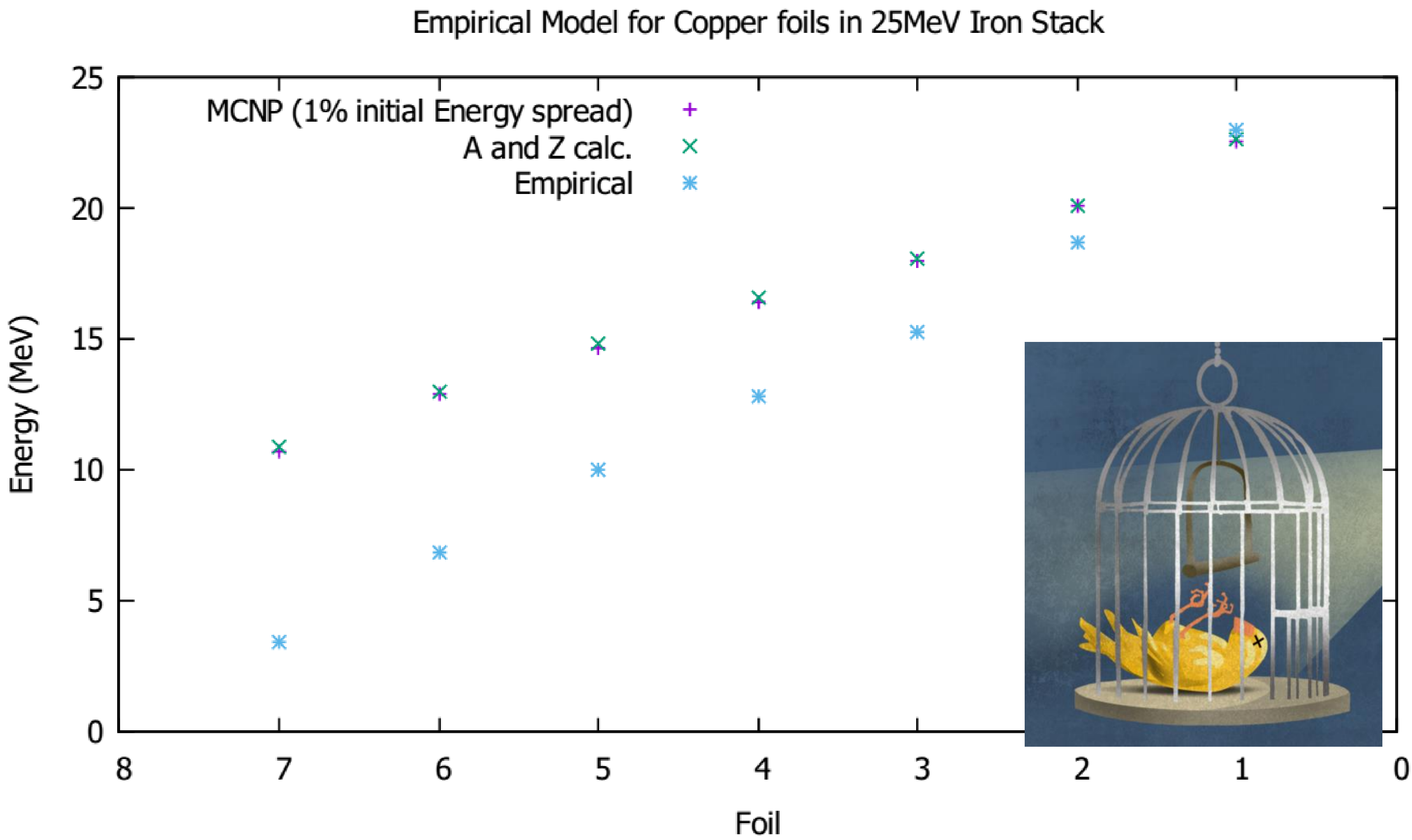
Empirical Model for Copper foils in 25MeV Iron Stack
MCNP (1% initial Energy spread)
A and Z calc.
Empirical
Energy (MeV)
Foil
0
5
10
15
20
25
8
7
6
5
4
3
2
1
0

Corrected Energy Assignments

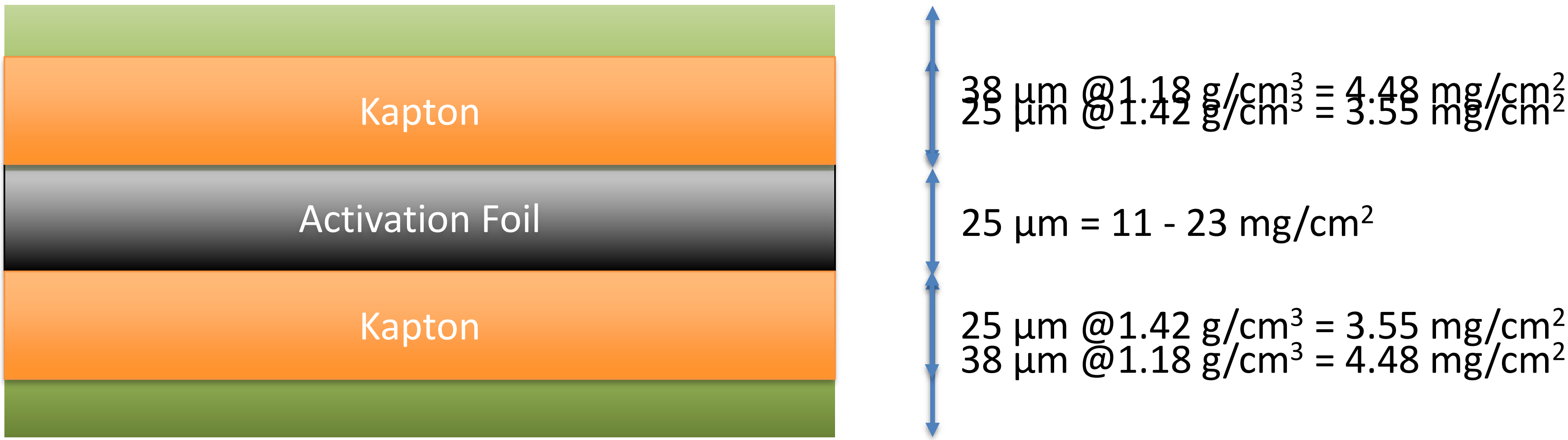

Corrected Energy Assignments

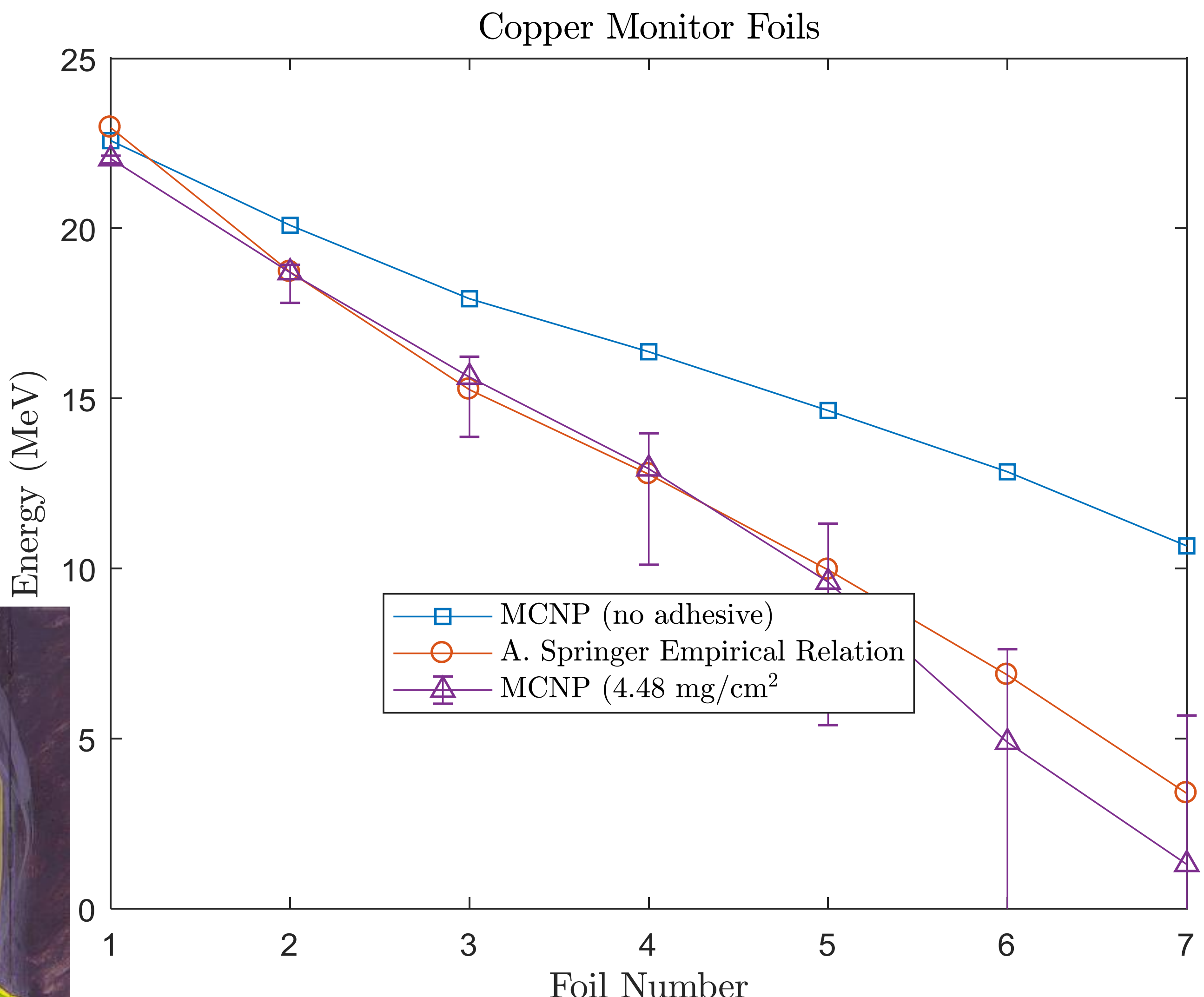

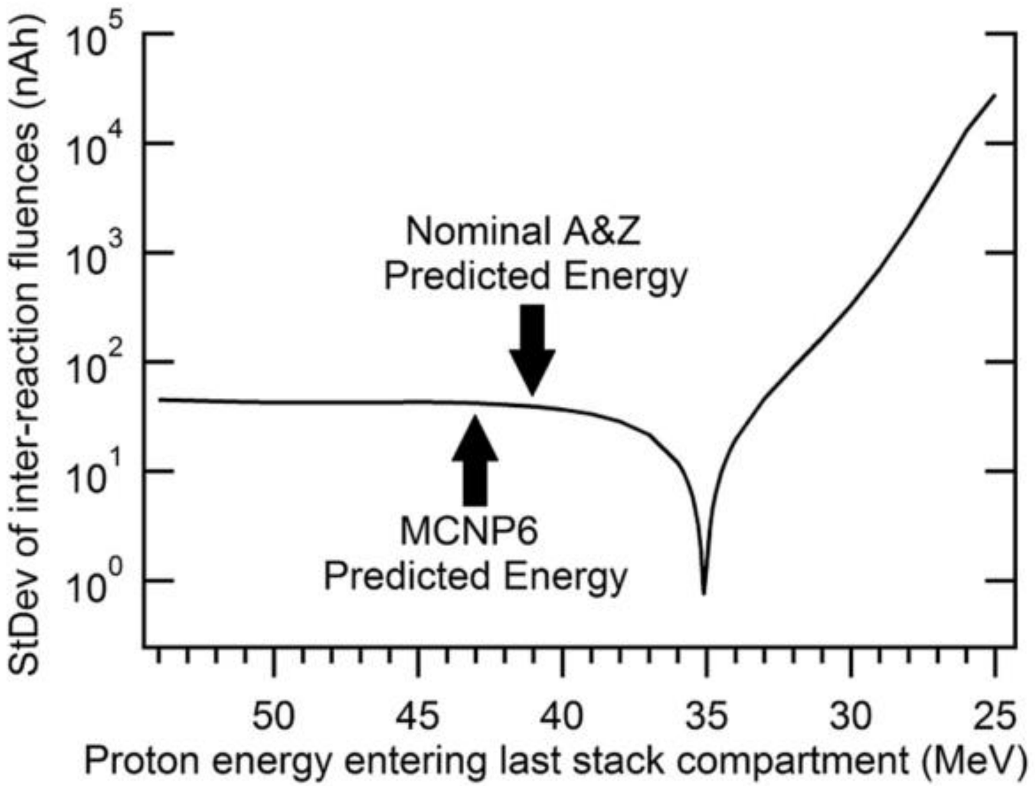

Fig. 3. Results of varying degrader density in analytic A&Z calculations on inter-monitor reaction fluence standard deviation. Varying degrader density has the effect of non-linearly varying the average beam energy in each compartment. This non-linear dependence on density has nearly the same functional impact as variations in the incident beam energy. Arrows indicate the predicted average beam energy in the last stack compartment by MCNP6 simulation and nominal A&Z calculations. A clear minimum from this approach is seen at 35.1 MeV, suggesting the initial beam energy estimations by nominal A&Z calculations and by MCNP6 simulation are significantly higher than what was experimentally observed.

LANL sees the same issue…

S. A. Graves, P. A. Ellison, T. E. Barnhart, H. F. Valdovinos, E. R. Birnbaum, F. M. Nortier, R. J. Nickles, and J. W. Engle, *Nucl. Instruments Methods Phys. Res. Sect. B Beam Interact. with Mater. Atoms*, vol. 386, pp. 44–53, Nov. 2016.

Corrected Energy Assignments

$$\chi = \frac{R_{prod}}{\int \sigma_{IAEA}(E) \frac{d\phi_{MCNP}}{dE} \rho \Delta r dE}$$

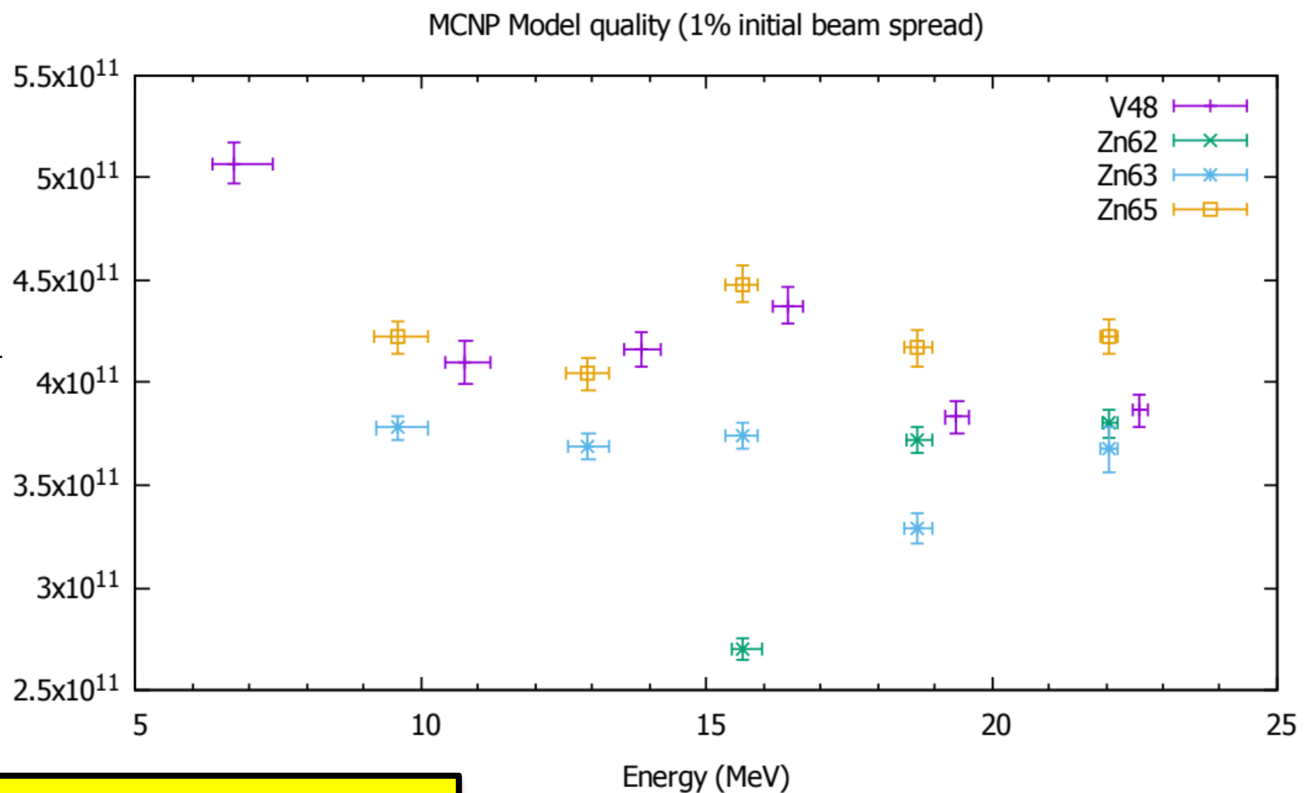

Goal: Minimize standard deviation of χ

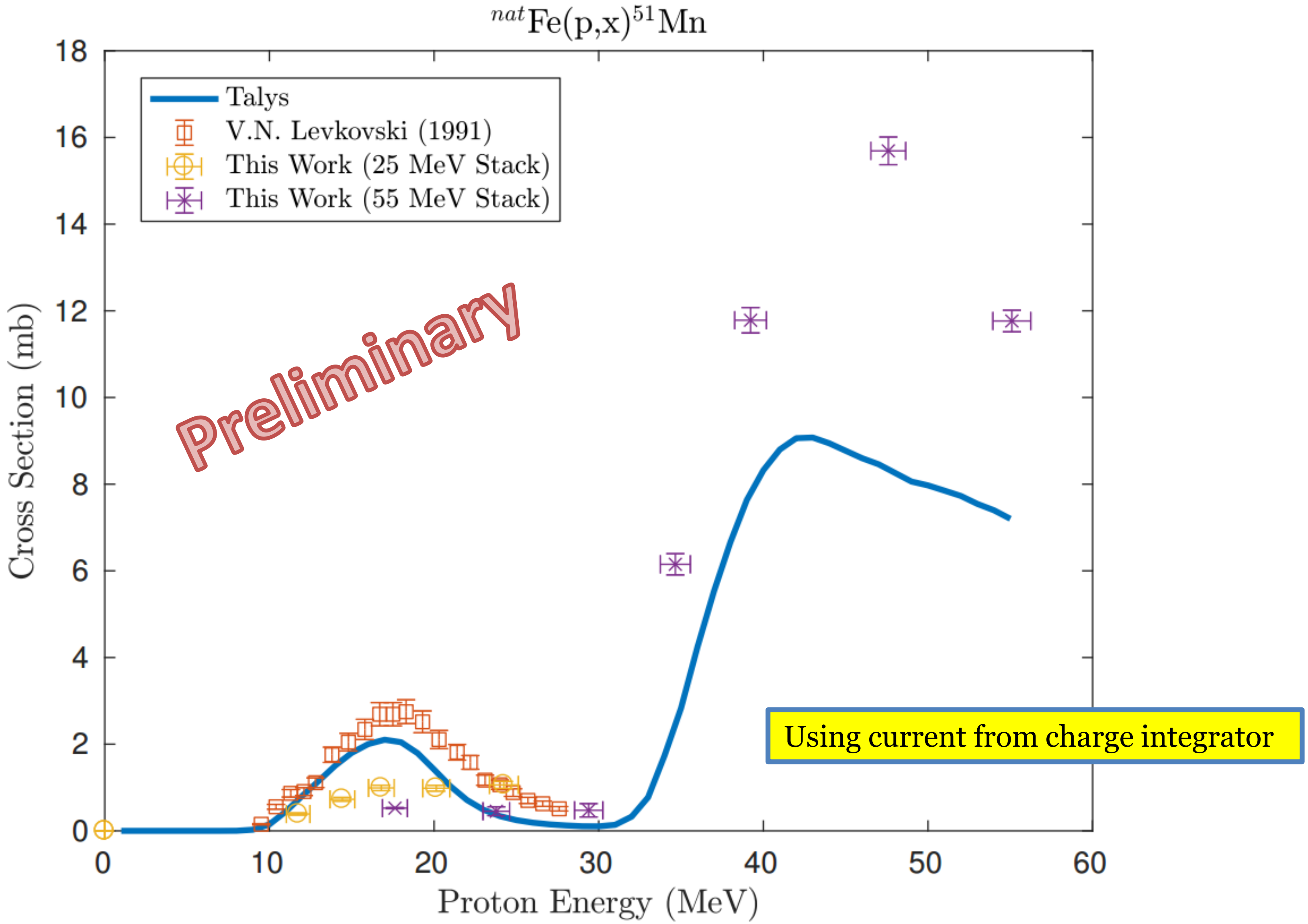
$^{nat}Fe(p,x)^{51}Mn$
Talys
V.N. Levkovski (1991)
This Work (25 MeV Stack)
This Work (55 MeV Stack)
Preliminary
Cross Section (mb)
Proton Energy (MeV)
0
2
4
6
8
10
12
14
16
18
0
10
20
30
40
50
60
Using current from charge integrator

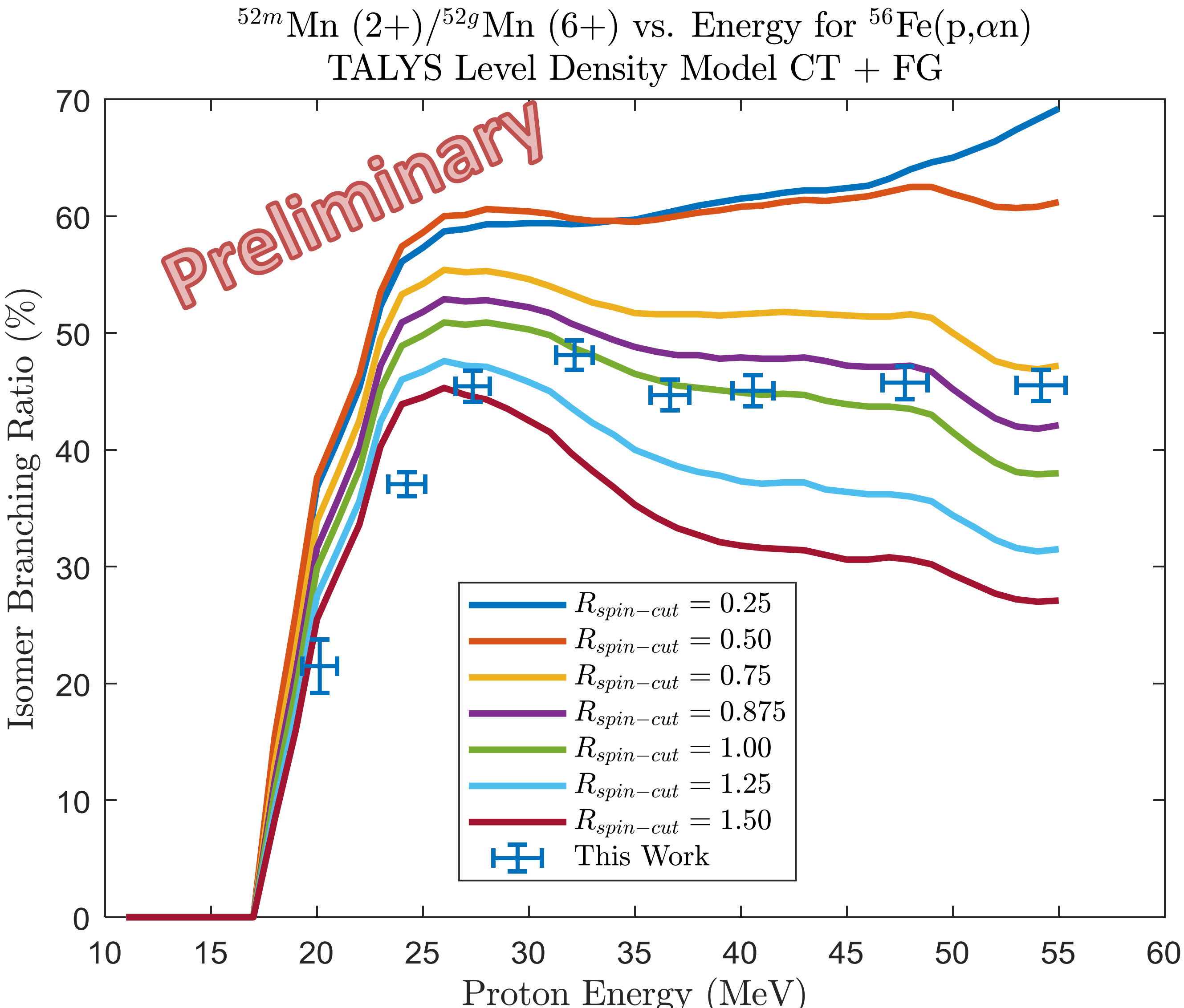

Results consistent with R≈1 at high energy.

At low energy, results are ambiguous due to energy straggling.

Spin Distribution Application

- Through its impact on nuclear level densities, the spin cut-off parameter has a strong impact on the favoring of higher-spin isomers in charged particle-induced reactions – a “tuning parameter” for isomer-to-ground state branching ratio
  - Reaction physics codes can be used to model (σ_m/σ_g) when experimental data is unavailable
  - Case study: ^{177}Lu
    - ^{177g}Lu ($t_{1/2}$ = 6.7 d) – emerging β^- therapy agent
    - ^{177m}Lu ($t_{1/2}$ = 160 d) – contributes extra dose to patient, without therapeutic or diagnostic benefit
    - Improved spin distribution measurements can improve modeling to guide production studies

Stacked-target Charged Particle Excitation Functions

Moderate Energy – LANL

Measurements @ LANL – Nb(p,x)

- $^{nat}Nb(p,4n)^{90}Mo$ is a high-priority objective as a new proton beam dosimetry standard for $E_p \approx 50 – 100$ MeV
  - Other emerging radionuclides: ^{82m}Rb, ^{86}Y, ^{89}Zr, ^{90}Nb

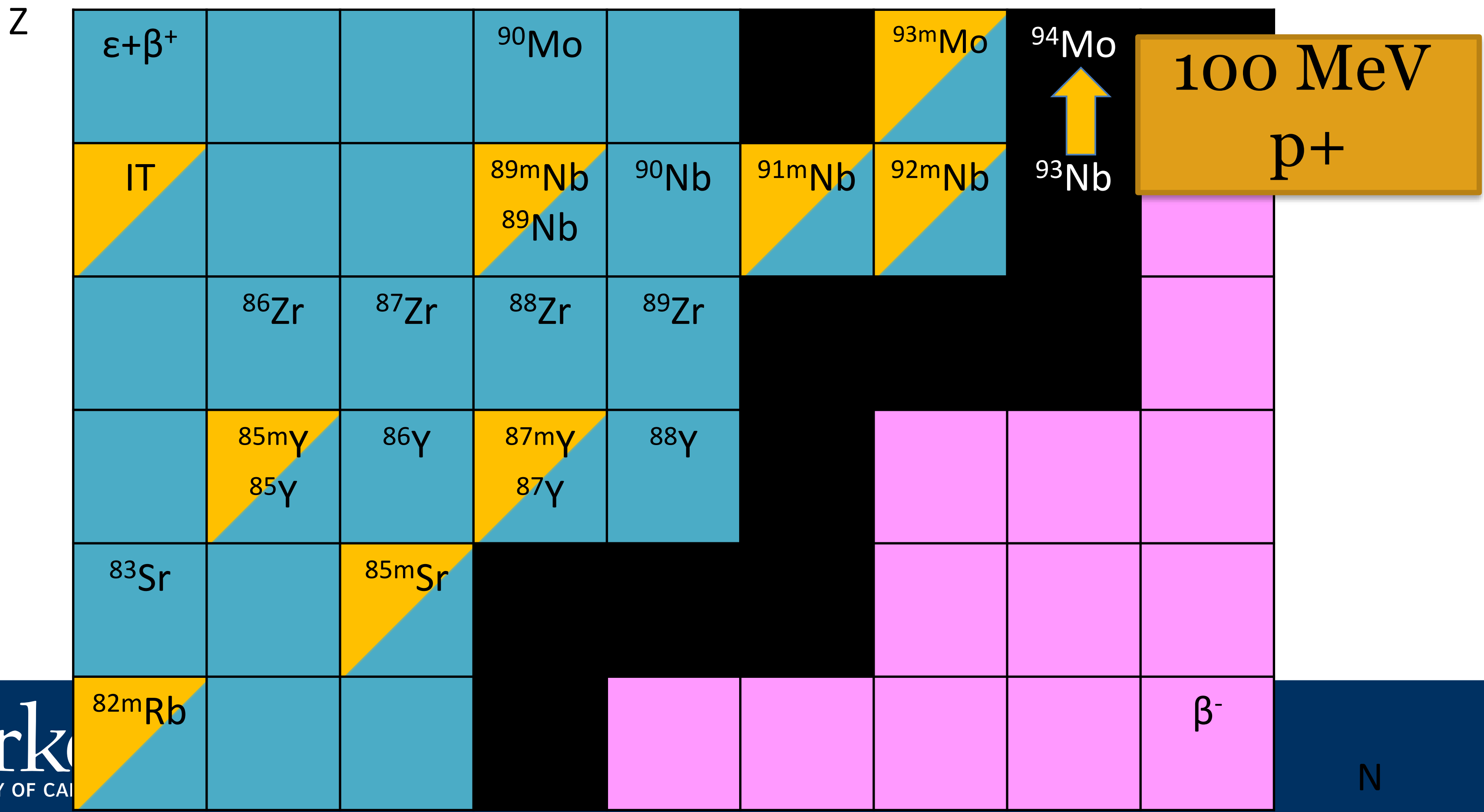

Measurements @ LANL – Nb(p,x)

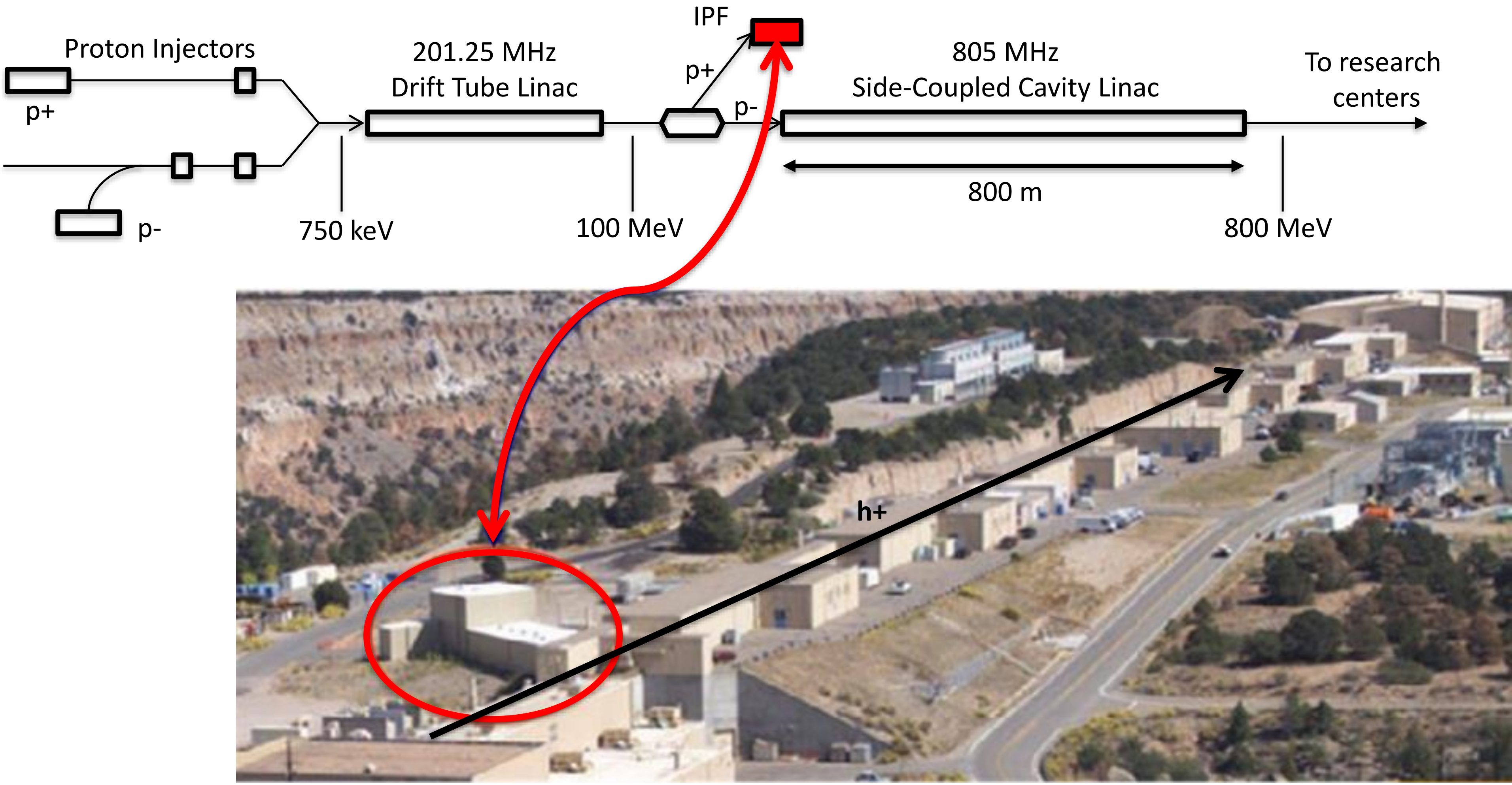

Measurements @ LANL – Nb(p,x)

- LBNL: 5 – 55 MeV / A, LANL: 45 – 100 MeV p^+
- Complementary measurements explore reaction dynamics in different energy regimes, overlap region of 45-55 MeV builds confidence and consistency in results.

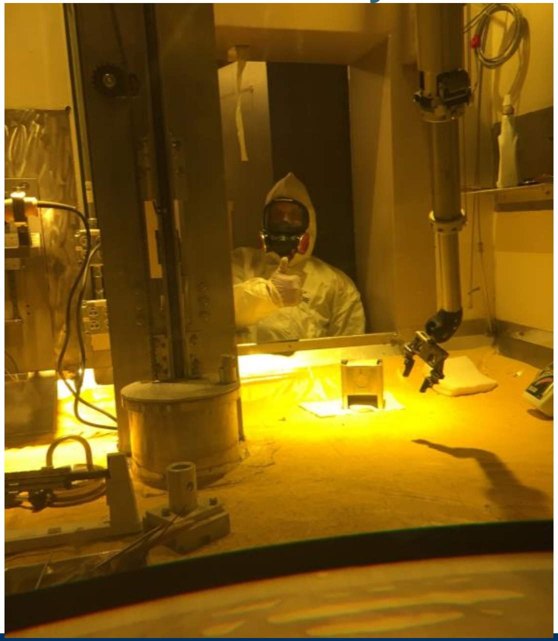

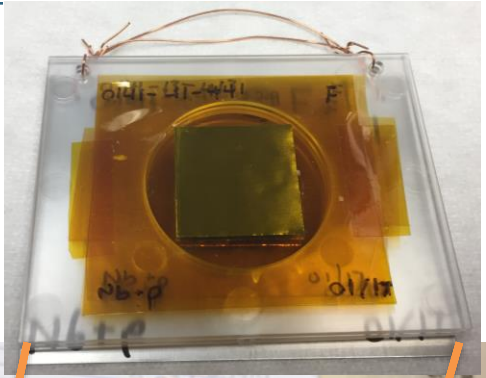

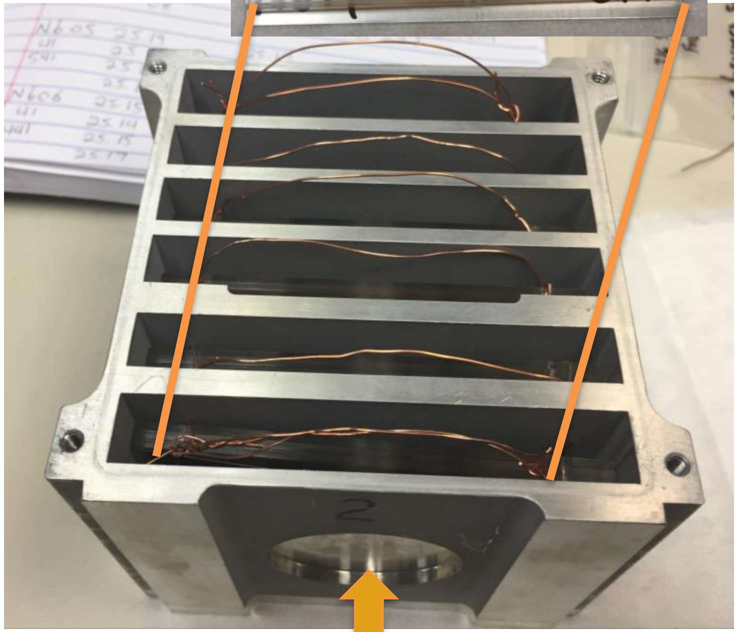

100 MeV p+

100 nA @ 3 hr

Measurements @ LANL – Nb(p,x)

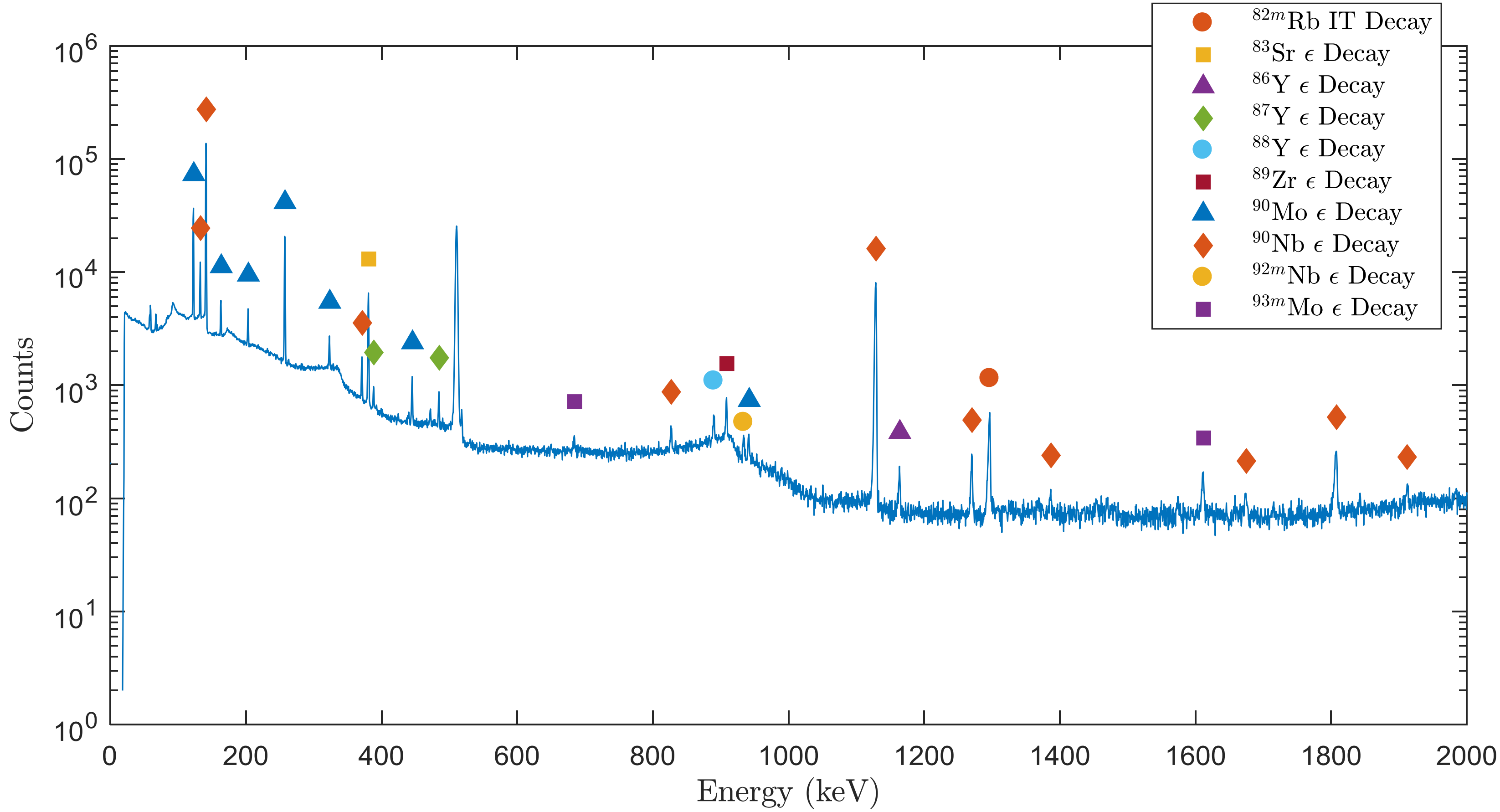

Measurements @ LANL – Nb(p,x)

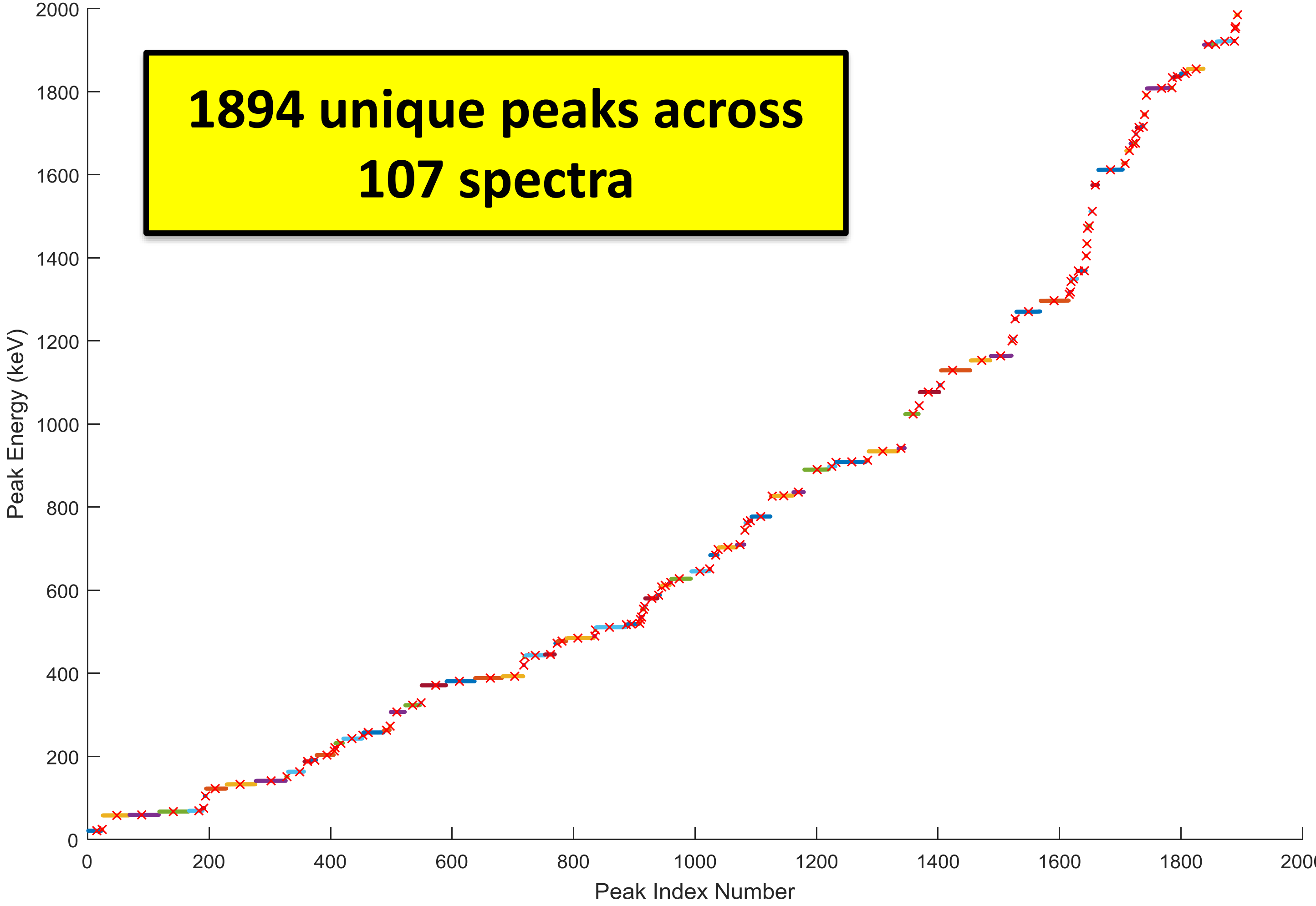

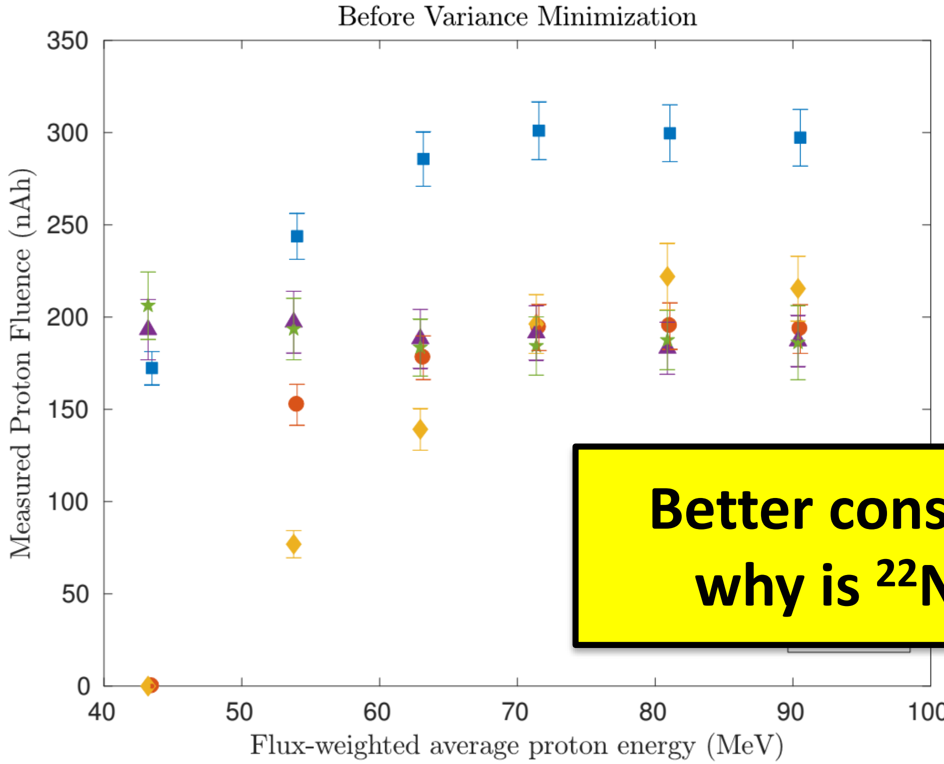

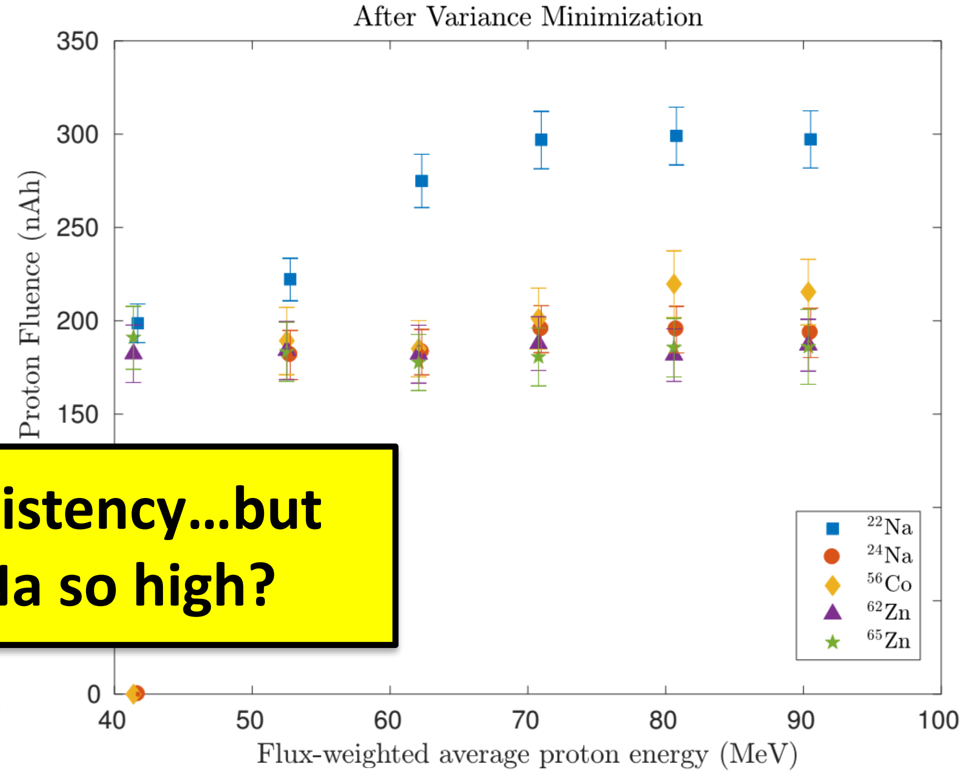

Better consistency…but why is ^{22}Na so high?

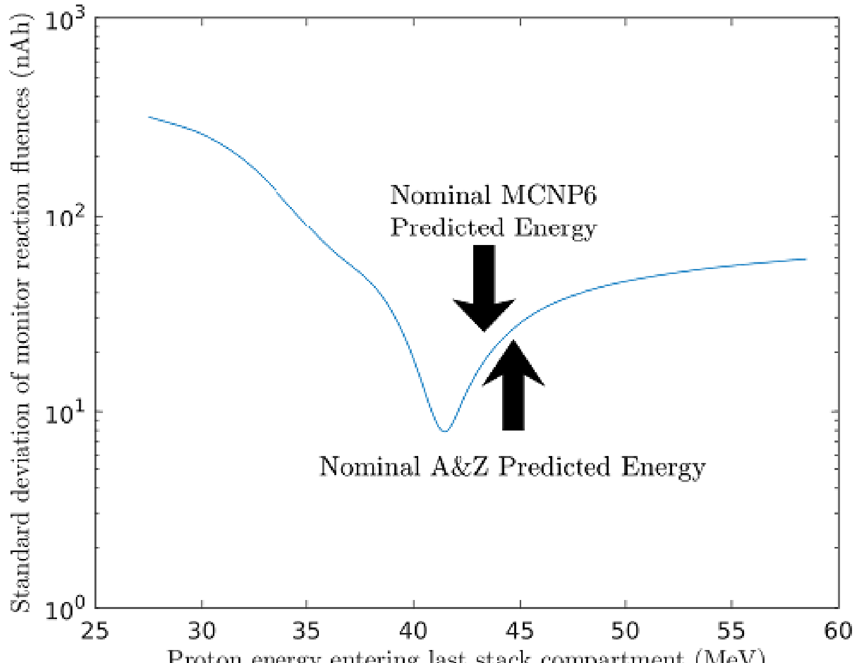

Berkeley
UNIVERSITY OF CALIFORNIA

It's always the Kapton!

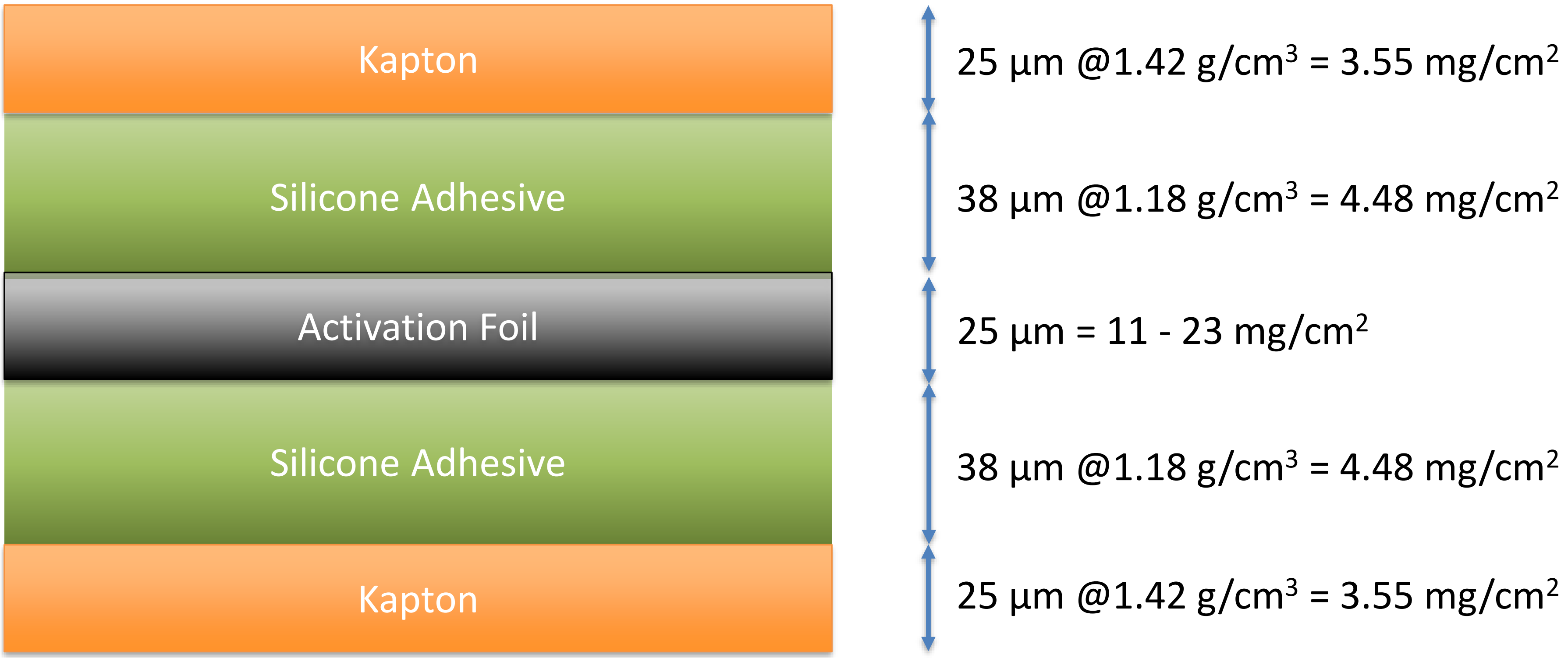

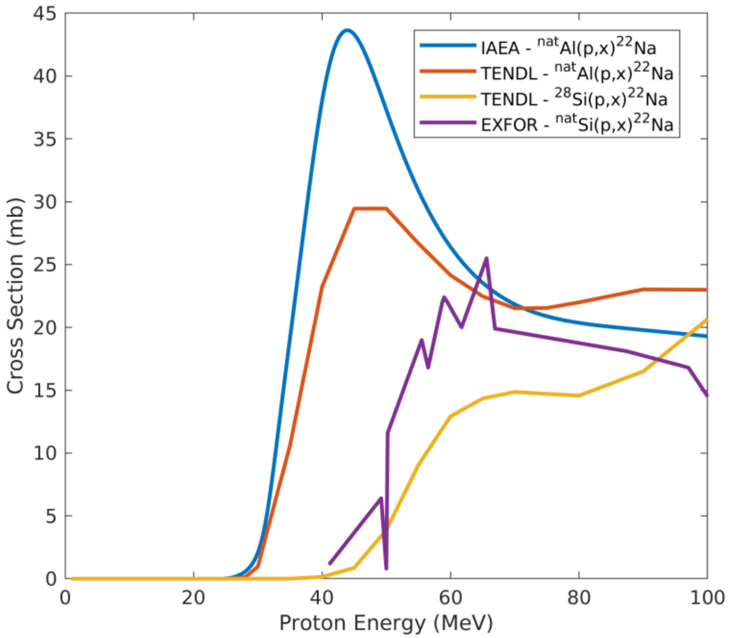
IAEA - natAl(p,x)22Na
TENDL - natAl(p,x)22Na
TENDL - 28Si(p,x)22Na
EXFOR - natSi(p,x)22Na
Cross Section (mb)
Proton Energy (MeV)

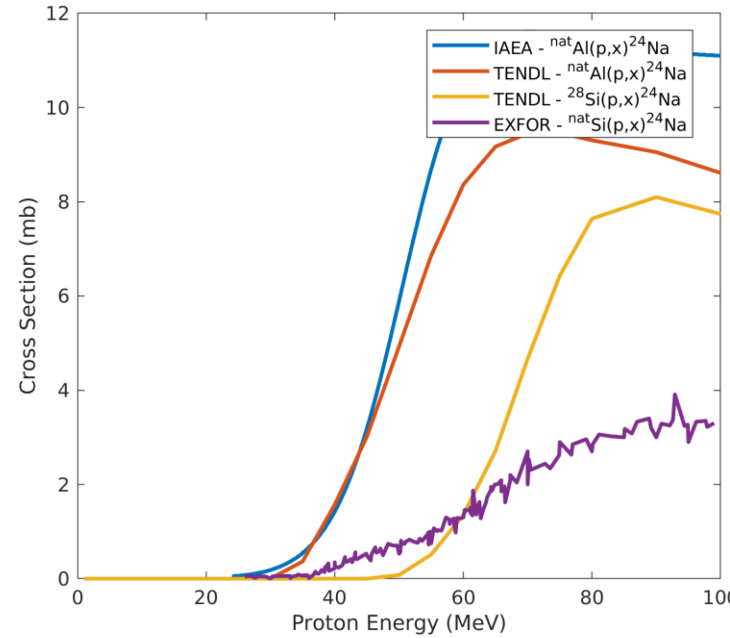
IAEA - natAl(p,x)24Na
TENDL - natAl(p,x)24Na
TENDL - 28Si(p,x)24Na
EXFOR - natSi(p,x)24Na
Cross Section (mb)
Proton Energy (MeV)

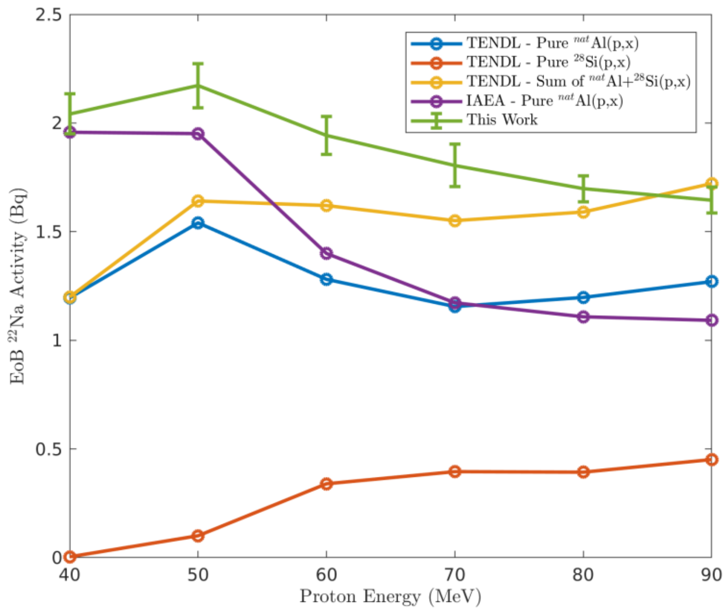
TENDL - Pure natAl(p,x)
TENDL - Pure 28Si(p,x)
TENDL - Sum of natAl+28Si(p,x)
IAEA - Pure natAl(p,x)
This Work
EoB 22Na Activity (Bq)
Proton Energy (MeV)

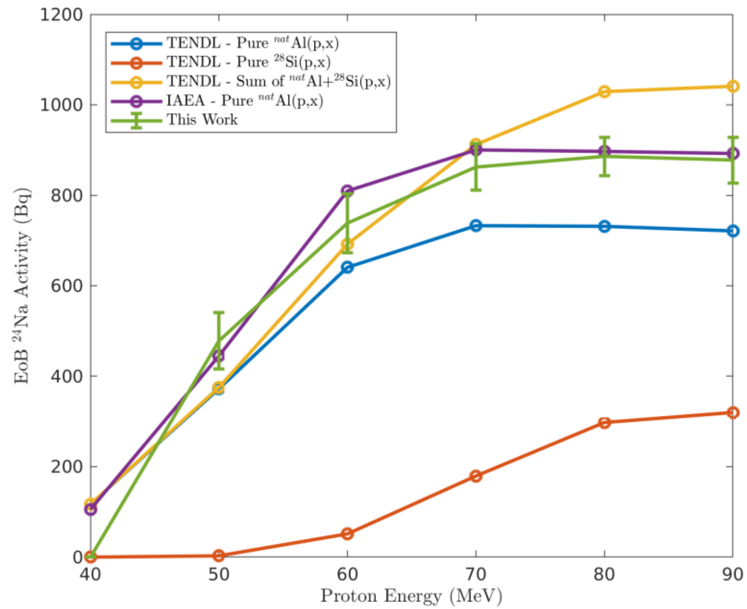
TENDL - Pure natAl(p,x)
TENDL - Pure 28Si(p,x)
TENDL - Sum of natAl+28Si(p,x)
IAEA - Pure natAl(p,x)
This Work
EoB 24Na Activity (Bq)
Proton Energy (MeV)

Measurements @ LANL – Nb(p,x)

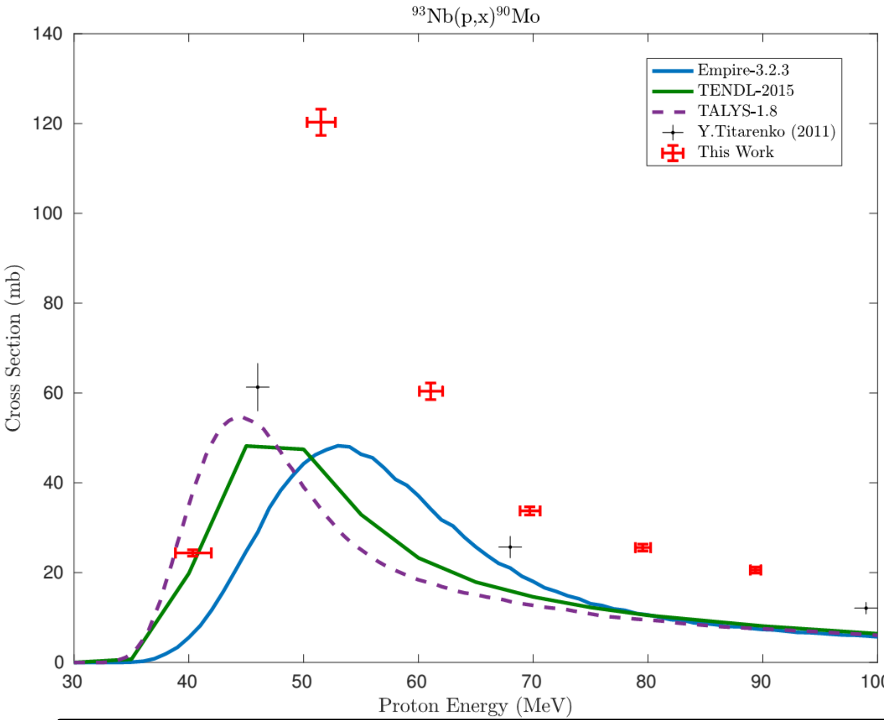

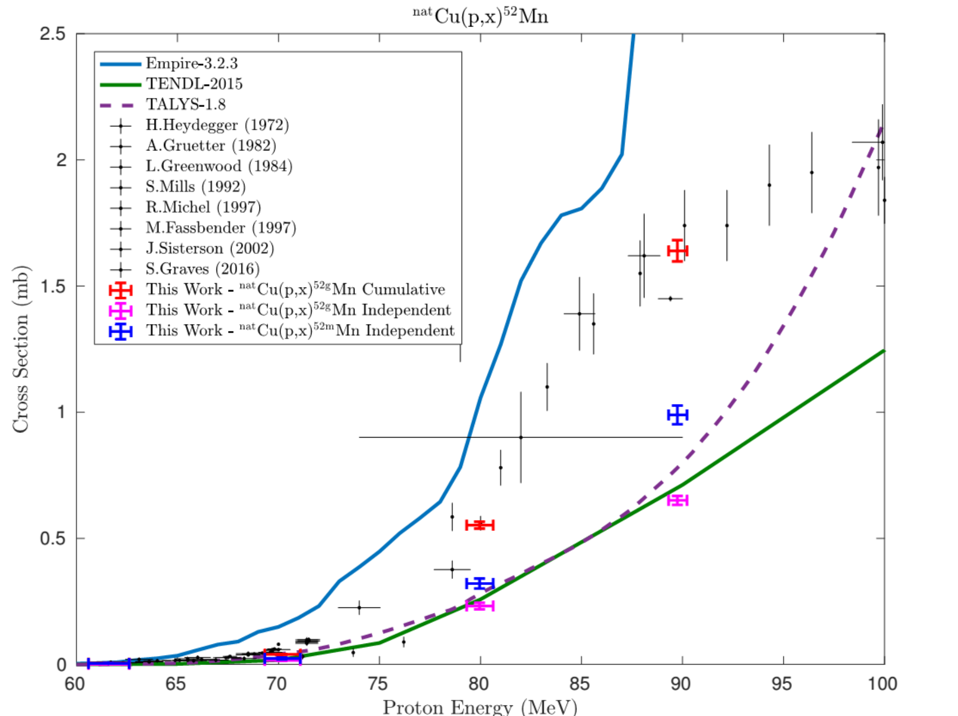

38 measurements of cross-sections for ^{93}Nb(p,x) and ^{nat}Cu(p,x)

Table 3. Measured cross sections for the various ^{nat}Nb(p,x) reaction products observed in this work. Cumulative cross sections are designated as σ_c, independent cross sections are designated as σ_i.

	Production cross section (mb)					
E_p (MeV)	$89.37^{+0.47}_{-0.45}$	$79.55^{+0.68}_{-0.64}$	$69.70^{+0.90}_{-0.85}$	$61.07^{+1.05}_{-0.98}$	$51.51^{+1.25}_{-1.21}$	$40.34^{+1.58}_{-1.55}$
^{82m}Rb (σ_c)	2.39 ± 0.18	–	–	–	–	–
^{83}Sr (σ_c)	3.88 ± 0.56	4.63 ± 0.34	3.42 ± 0.32	–	–	–
^{85}Y (σ_c)	13.31 ± 0.30	7.28 ± 0.44	2.06 ± 0.12	–	–	–
^{85g}Y (σ_i)	2.286 ± 0.057	2.01 ± 0.15	0.545 ± 0.030	–	–	–
^{85m}Y (σ_i)	11.03 ± 0.30	5.27 ± 0.42	1.52 ± 0.12	–	–	–
^{86}Zr (σ_c)	12.25 ± 0.32	17.63 ± 0.44	18.86 ± 0.43	6.00 ± 0.15	–	–
^{86}Y (σ_i)	32.25 ± 0.89	40.3 ± 1.1	39.0 ± 1.0	13.22 ± 0.34	–	–
^{87}Zr (σ_c)	45.8 ± 5.8	27.1 ± 1.7	31.5 ± 1.5	48.5 ± 2.9	37.7 ± 1.6	1.13 ± 0.10
^{87}Y (σ_i)	106.3 ± 5.8	52.9 ± 1.7	59.6 ± 1.5	87.8 ± 2.9	66.3 ± 1.6	2.93 ± 0.10
^{87g}Y (σ_i)	27.0 ± 5.4	7.1 ± 1.2	6.41 ± 0.55	5.6 ± 2.1	2.59 ± 0.45	0.949 ± 0.045
^{87m}Y (σ_i)	79.2 ± 2.0	45.8 ± 1.2	53.2 ± 1.4	82.1 ± 2.0	63.7 ± 1.5	1.983 ± 0.093
^{88}Zr (σ_c)	153.7 ± 3.9	140.0 ± 3.5	61.0 ± 1.7	20.65 ± 0.49	33.16 ± 0.97	65.8 ± 1.3
^{88}Y (σ_i)	16.64 ± 0.76	12.85 ± 0.60	7.81 ± 0.61	2.83 ± 0.20	9.0 ± 1.3	9.96 ± 0.33
^{89}Nb (σ_c)	–	–	176 ± 12	209.0 ± 4.3	–	–
^{89g}Nb (σ_i)	–	–	142 ± 12	181.7 ± 4.1	–	–
^{89m}Nb (σ_i)	–	–	33.9 ± 2.0	27.3 ± 1.4	–	–
^{89}Zr (σ_i)	203.8 ± 5.3	235.4 ± 6.6	287.5 ± 6.8	250.3 ± 5.8	54.6 ± 1.1	15.61 ± 0.31
^{90}Mo (σ_c)	20.6 ± 0.7	25.58 ± 0.76	33.75 ± 0.90	60.4 ± 1.9	120.3 ± 2.9	24.38 ± 0.71
^{90}Nb (σ_i)	152.9 ± 4.7	169.3 ± 4.8	204.7 ± 5.8	265.2 ± 7.8	363.4 ± 9.8	165.2 ± 4.5
^{91m}Nb (σ_c)	–	–	–	–	–	67.0 ± 4.2
^{92m}Nb (σ_c)	42.2 ± 1.2	45.7 ± 1.2	48.8 ± 1.2	51.6 ± 1.3	54.5 ± 1.4	60.4 ± 1.2
^{93m}Mo (σ_c)	0.93 ± 0.18	1.25 ± 0.13	1.58 ± 0.22	1.80 ± 0.12	1.83 ± 0.10	2.010 ± 0.084

A.S. Voyles *et al.*, "Measurement of nuclear excitation functions for proton induced reactions (E_p = 40 – 90 MeV) on natural Nb and Cu", PRC 2018 (in preparation)

Measurements @ LANL – Nb(p,x)

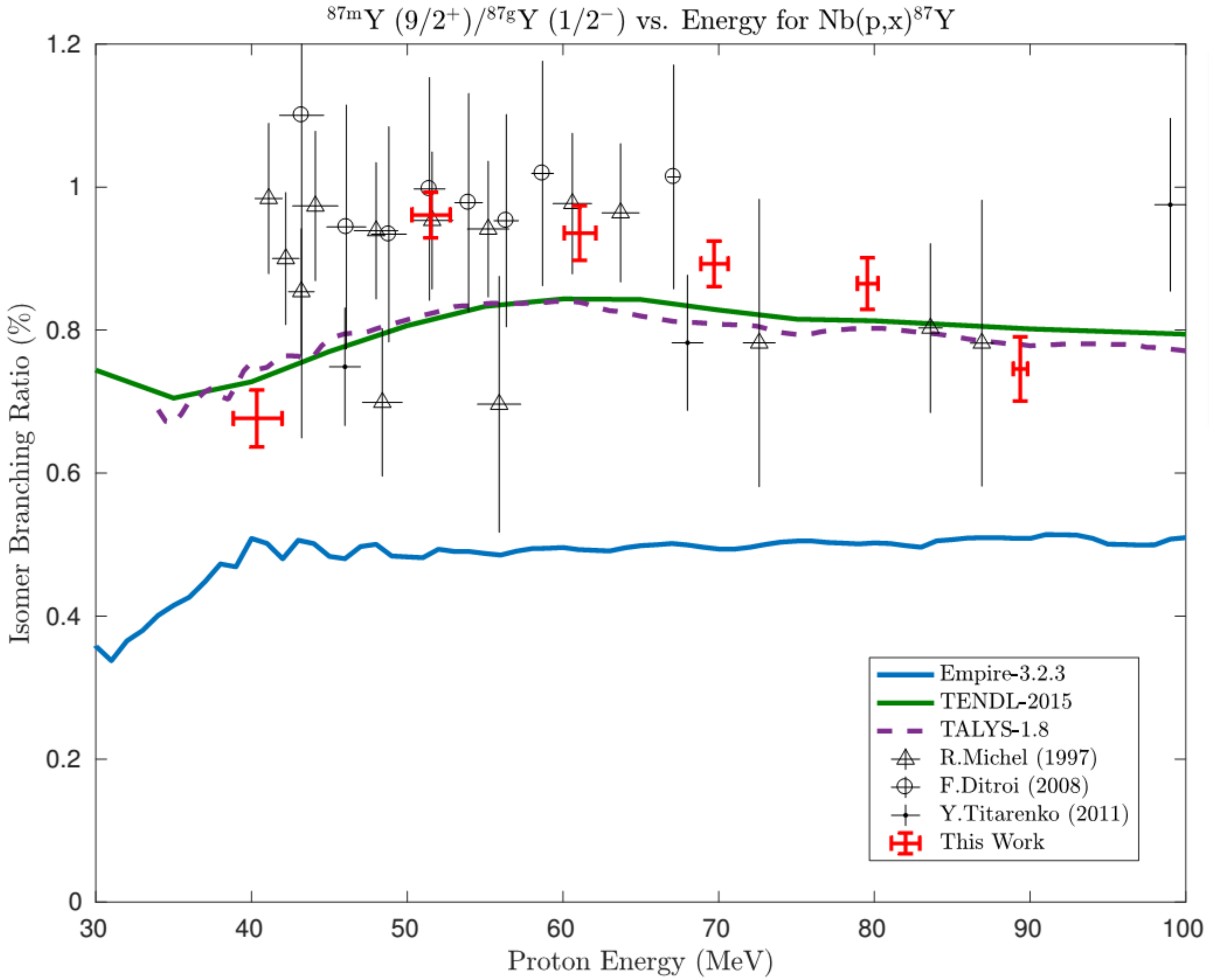

5 independent measurements of isomer-to-ground state ratios

A. Lewis

Demonstrated ability to measure excitation functions for emerging medical radionuclides through 3 different production paradigms

- Provides first / vastly improved production measurements for each of the isotopes listed here
- Thin-target measurements in this work provide an ideal jumping-off point to begin thick-target yields for commercial application, as well as radiochemical workup

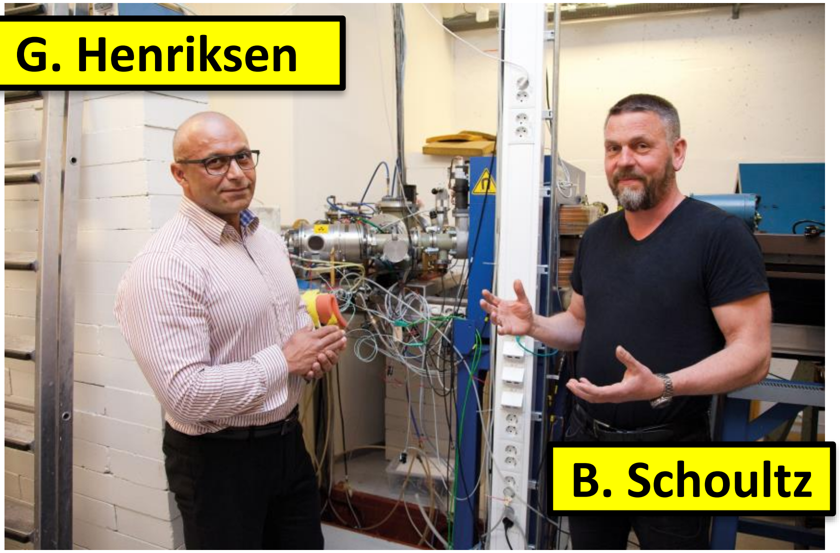

Path Forward: $^{238}U(p,xn)^{236,237}Np$ and $^{235}U(d,x)^{236}Np$ Production

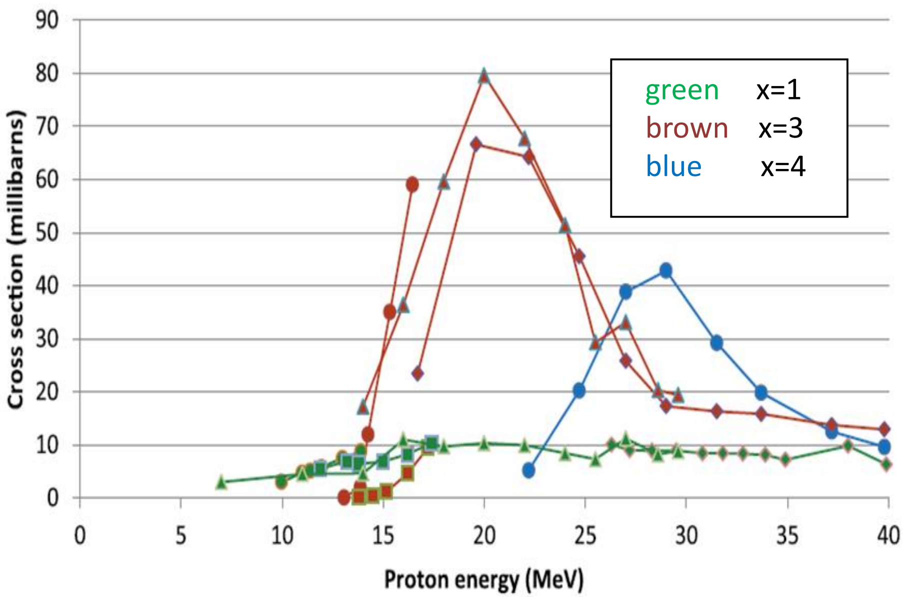

Literature reaction cross sections for $^{238}U(p, xn)$

Vital mass-spec "spike" for nonproliferation

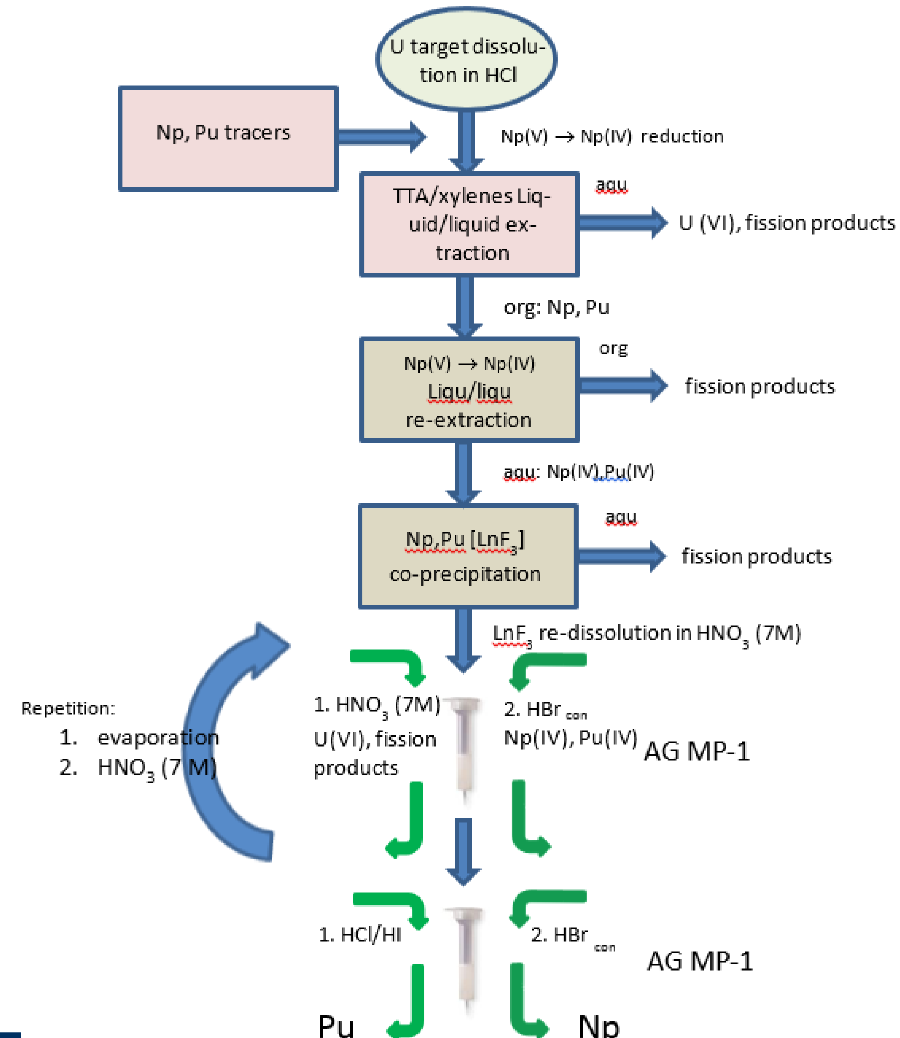

Path Forward:
^{7}Li(p,n) "Quasi-Monoenergetic" Neutron Source

Vault-based irradiation

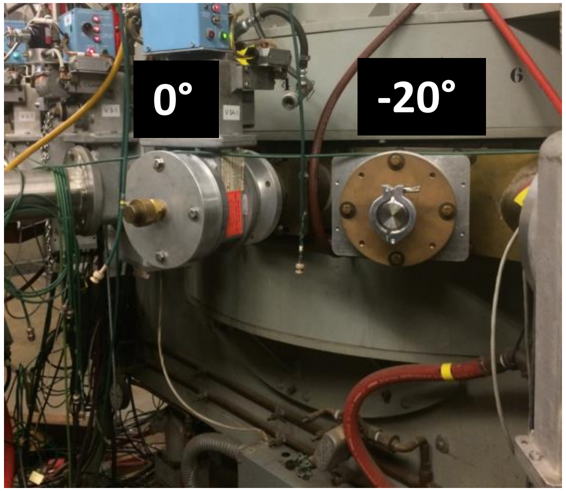

Inconel-clad Li targets
(LANL LDRD)

Jon Engle

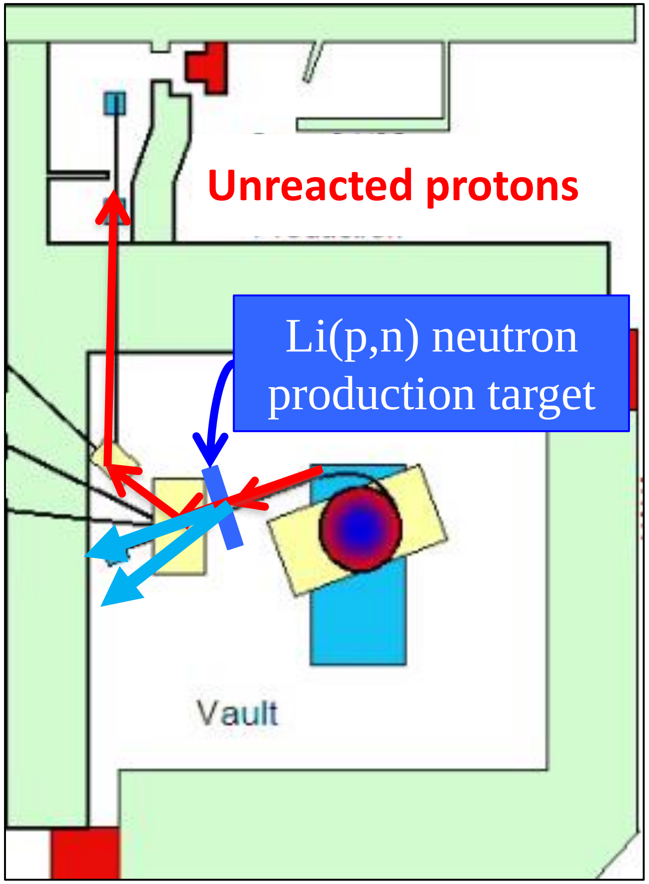

- Neutrons from 0-***60*** MeV
- Samples irradiated in the vault
- Unreacted beam dumped in Cave 0
- Flux from 10^{6-4} /MeV/sr/s (decreases w/E_n)

First experiments are planned for April 2018

Path Forward: ^{140}La(p,6n)^{134}Ce as a PET tracer for ^{225}Ac

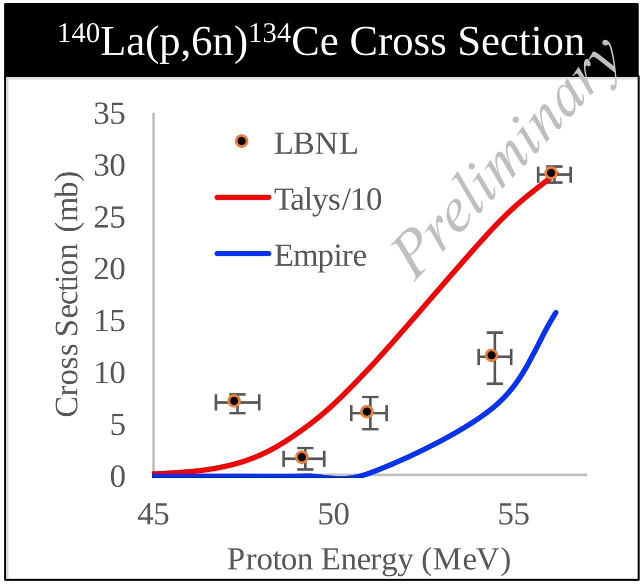

Stacked Target Holder

HPGe counter

Jon Morrell

Investigating potential for ^{226}Ra(2,2n)^{225}Ra → ^{225}Ac

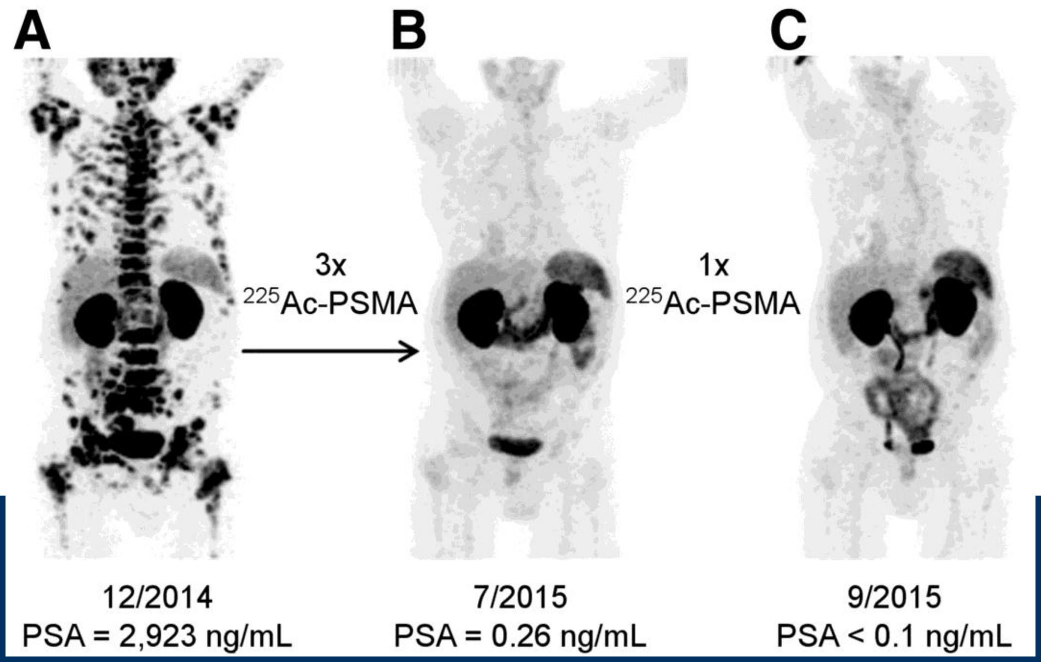

Kratochwil, Clemens, et al. "225Ac-PSMA-617 for PSMA-targeted α-radiation therapy of metastatic castration-resistant prostate cancer." *Journal of Nuclear Medicine* 57.12 (2016): 1941-1944.

Collaborators on this work

M.S. Basunia[1], J.A. Batchelder[2], J.D. Bauer[3], T.A. Becker[4], L.A. Bernstein[1,2], E.R. Birnbaum[5], J.W. Engle[5,6], R.B. Firestone[1], S.A. Graves[7], G. Henriksen[8], A.M. Hurst[1], L. Kirsch[3], A.M. Lewis[2], E.F. Matthews[2], F.M. Nortier[5], S.M. Qaim[9], P.R. Renne[4], D. Rutte[4], B.W. Schoultz[10], S. Siem[11], A. Springer[12], M.A. Unzueta[2], K.A. Van Bibber[2], A.S. Voyles[2], C.S. Waltz[3] H. Zaneb[13]

[1] *Lawrence Berkeley National Laboratory*
[2] *University of California-Berkeley Dept. of Nuclear Engineering*
[3] *Lawrence Livermore National Laboratory*
[4] *Berkeley Geochronology Center*
[5] *Los Alamos National Laboratory*
[6] *University of Wisconsin – Madison*
[7] *University of Iowa – Department of Radiation Oncology*
[8] *University of Oslo – Institute of Basic Medical Sciences*
[9] *Forschungszentrum Jülich*
[10] *University of Oslo – Department of Chemistry*
[11] *University of Oslo – Department of Physics*
[12] *Karlsruhe Institute of Technology*
[13] *University of Lahore*